Positive and Negative Modulation of Group I Metabotropic Glutamate Receptors

Maksims Vanejevs,[†] Claudia Jatzke,[‡] Steffen Renner,[‡] Sibylle Müller,[‡] Mirko Hechenberger,[‡] Tanja Bauer,[‡] Anna Klochkova,[§] Ilya Pyatkin,[§] Denis Kazyulkin,[§] Elena Aksenova,[§] Sergey Shulepin,[§] Olga Timonina,[§] Ariane Haasis,[‡] Aleksandrs Gutcaits,[†] Christopher G. Parsons,[‡] Valerjans Kauss,[†] and Tanja Weil*,[‡]

Institute of Organic Synthesis, 21 Aizkraukles Street, Riga, LV1006, Latvia, Merz Pharmaceuticals GmbH, Altenhöferallee 3, D-60438 Frankfurt am Main, Germany, and Asinex Ltd., 5 Gabrichevskogo Street, Building 8, Moscow 125367, Russia

Received September 28, 2006

A discriminating pharmacophore model for noncompetitive metabotropic glutamate receptor antagonists of subtype 1 (mGluR1) was developed that facilitated the discovery of moderately active mGluR1 antagonists. One scaffold was selected for the design of several focused libraries where different substitution patterns were introduced. This approach facilitated the discovery of potent mGluR1 antagonists, as well as positive and negative mGluR5 modulators, because both receptor subtypes share similar binding pockets. For mGluR1 antagonists, a homology model of the mGlu1 receptor was established, and a putative binding mode within the receptor's transmembrane domain was visualized.

Introduction

G protein-coupled receptors (GPCRs) represent a large protein superfamily that plays an important role in many physiological and pathophysiological processes. In the past, the discovery of molecules acting at GPCRs has been extremely successful with about 50% of all recently launched drugs targeting GPCRs.[1] Metabotropic glutamate receptors (mGluRs),[2] together with parathyroid calcium sensing receptors (CaSR),[3] γ-aminobutyric acid type B receptors ($GABA_BR1$ and $GABA_BR2$),[4,5] some vomeronasal receptors (V2Rs),[6] taste receptors (T1R1–3),[7] and putative pheromone receptors,[8] belong to family C GPCRs. mGluRs mediate excitatory transmission on the cellular surface through initial binding of glutamate, thus influencing the strength of synaptic transmission.[9,10] The mGluR family comprises eight subtypes with several splice variants, which have been named mGluR1–8 according to the succession of the molecular cloning.[11] These eight receptors are further subdivided into three groups on the basis of their sequence homology, pharmacology, and transduction mechanism: Group I (mGluR1 and mGluR5),[a] group II (mGluR2 and mGluR3), and group III (mGluR4, mGluR6, mGluR7, and mGluR8).[11] A structural characteristic of mGluRs is their large extracellular domain where the natural ligand glutamate, as well as competitive agonists and antagonists, bind.[11,12] The transmembrane domain (TM) bears binding sites of allosteric modulators, which in general are considered more selective than competitive ones.[13] mGluR1 and mGluR5 are primarily localized postsynaptically.[11] They are widely distributed in many brain regions, including the hippocampus, cerebellum, thalamic nuclei, and spinal cord.[14] Stimulation of mGluR1 and mGluR5 leads to phosphoinositide (PI) hydrolysis and elevation of intracellular calcium levels via coupling of Gα q/11-protein to phospholipase C.[15,16] According to the previous studies, the mGluR1 receptor seems to be mainly involved in therapeutic opportunities such as stroke,[42] brain injury,[17] and pain.[18] Excessive activation of mGluR5 receptors has been implicated in a number of central nervous system disorders including pain,[19] anxiety,[20] depression,[20] other neurological impairments such as drug addiction,[21] and Parkinsons disease.[22]

Therefore, antagonists of mGluR5 could be of interest for these indications. In contrast, the selective activation of mGluR5 via positive modulators could normalize hypofunctional activity mediated *via* N-methyl-D-aspartate (NMDA) receptors, and could therefore be of interest for the development of novel antipsychotic drug treatments.[23,24]

In the past, some potent antagonists and positive modulators of mGluR1 and mGluR5 have been described.[25] However, the discovery of novel mGluR modulators via ligand-based or structure-based virtual screening techniques is often limited because of the lack of structurally diverse ligands, as well as the low sequence identity of mGluRs and bovine rhodopsin, which was at the time the studies were performed, the only example of a successfully crystallized GPCR.[26] To date, the discovery of novel mGluR modulators is mainly based on high-throughput screening (HTS) approaches, which bear inherent drawbacks such as high cost and a high number of false-positive or -negative hits.[27] Therefore, we first focused on the development of a pharmacophore hypothesis for allosteric mGluR1 antagonists because, here, some structurally different ligands have been reported before.[25] Since the TM binding sites of mGluR1 and mGluR5 modulators reveal a high structural similarity ("partial overlap"), the discovery of a new mGluR1 allosteric modulator could potentially serve as a reasonable starting point for the development of novel mGluR5 modulators.[28] On the basis of the mGluR1 pharmacophore hypothesis, a small library was bought and screened for both mGluR1 and mGluR5 receptor subtypes. This approach allowed the discovery of weakly active mGluR1 antagonists. Among those, one novel scaffold was selected and chemically modified leading to highly potent negative modulators of mGluR1 and both positive and negative modulators of mGluR5. In addition, the putative binding mode of such a novel mGluR1 antagonist was visual-

* To whom correspondence should be addressed. E-mail: Tanja.Weil@merz.de. Fax: +49691503188. Phone: +49691503478.

† Institute of Organic Synthesis.

‡ Merz Pharmaceuticals GmbH.

§ Asinex Ltd.

[a] Abbreviations: EL2, extracellular loop 2; EM-TBPC, 1-ethyl-2-methyl-6-oxo-4-(1,2,4,5-tetrahydro-benzo[d]azepin-3-yl)-1,6-dihydro-pyrimidine-5-carbonitrile; FLIPR, fluorescent imaging plate reader; HQ, hydroquinolinone; [^{3}H]MPEP, [^{3}H]-2-methyl-6-(phenylethynyl)-pyridine; IP3, inositol-1,4,5-trisphosphat or inositoltriphosphate; mGluR1, metabotropic glutamate receptor 1; mGluR5, metabotropic glutamate receptor; TM, transmembrane.

10.1021/jm0611298 CCC: $40.75
Published on Web 01/04/2008

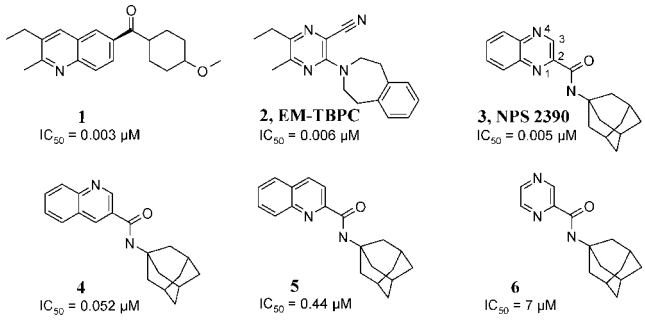

Figure 1. 2D-Structures and activity data of published mGluR1 antagonists.

ized, and the herein obtained structure–activity information (SAR) was interpreted by application of this homology model.

Results and Discussion

Pharmacophore Hypothesis of mGluR1. The first goal was directed toward the identification of novel mGluR1 antagonists from commercially available compound libraries. For this purpose, known mGluR1 antagonists were collected from public sources, and three structurally different antagonists were chosen for the development of an initial pharmacophore hypothesis. Compounds **1**,[29] **2**,[30] and **3**[31] (Figure 1) represent highly potent antagonists, and they were characterized in functional assays by detection of intracellular IP3 changes[32] (Experimental Section). To improve our understanding of the active conformation of these known antagonists and to assess the number of essential hydrogen bond acceptors, three derivatives of **3**, model compounds **4**, **5**, and **6** (Figure 1), were synthesized. These compounds revealed less potency for mGluR1: **4** was found to be about 10-fold less active than **3**, and **5** was found to be about 10-fold less active than **4** and about 100-fold less active than **3**. These first results already pointed toward a qualitatively greater importance of the N-acceptor group of position 4 versus position 1 of NPS 2390 (**3**, Figure 1). A reduction of the size of the aromatic ring system, for example, from quinoxaline (**3**) to pyrazine (**6**), gave a considerable decrease in activity. On the basis of these results, a flexible alignment of mGluR1 antagonists **1**, **2**, and **3** was accomplished by application of the software MOE (Chemical Computing Group, Figure 2a).

From this alignment, a pharmacophore hypothesis was created (Figure 2b, protocol is given in the Experimental Section). *Essential* groups within this pharmacophore query represent such groups that are mandatory in the output structure, whereas the presence of an *optional* group is not obligatory. Then, a data set consisting of about 250 000 structurally diverse compounds from the *Asinex Gold Collection*[33] was virtually screened by application of this pharmacophore model, and 39 compounds were purchased and investigated in a functional mGluR1 assay to detect changes in the IP3 level,[32] in addition to being used in a binding mGluR5 assay by displacement of the known mGluR5 antagonist [^{3}H]-2-methyl-6-(phenylethynyl)-pyridine[34] ([^{3}H]MPEP, Experimental Section). Four compounds with an mGluR1 IC_{50} below 10 μM were identified, corresponding to a hit rate of about 10%. Among these hits, **10a** represents a moderately potent mGluR1 antagonist with a hydroquinolinone (HQ) scaffold whose binding to mGluRs has not been reported before (Figure 2a). Furthermore, this scaffold offers the application of parallel synthesis methods for the straightforward design of further HQ derivatives.

Synthesis of a HQ library. For the sake of clarity, Figure 2a depicts a sketch of the relative orientation of hit compound **10a** with respect to the three-dimensional alignment of **1**, **2**, and **3**. According to the alignment of **10a** and the assignment of all pharmacophore features substituents at position 1 and 2 of the HQ scaffold were considered crucial for achieving mGluR1 potency. Therefore, a small library was designed where first R^1 was varied in a systematic way (Scheme 1). For R^2, the cyano substituent of **10a** was kept, whereas for R^3, either hydrogen or methyl groups were introduced (Tables 1 and 2). Compounds corresponding to the general formula **Ia** with a thioether linker (Scheme 1) were obtained from the 5-oxo-2-thioxo-1,2,5,6,7,8-hexahydro-quinoline-3-carbonitrile derivatives **8**, which in turn were prepared from cyclohexane-1,3-diones **7** according to published procedures.[35,36] Alkylation of **8** with alkyl halides, for example **9**, under basic conditions led to 2-alkylsulfanyl-5-oxo-5,6,7,8-tetrahydro-quinoline-3-carbonitriles (**10**) of the general formula **Ia** bearing a thioether linker. The synthesis of all main products is given in the Experimental Section. Compound **12** represents a key building block for the introduction of amino substituents. The reactive chloro group at position 1 was gained after reaction of **11**[36,37] with phosphoryl chloride in moderate yields;[38] **12a/b** then underwent substitution reactions with a library of appropriately functionalized amino derivatives in moderate to excellent yields (**14,** general formula **Ib**). All substituents R^1 that were introduced via the above-mentioned procedure are given in Table 1.

A synthetic procedure toward HQs carrying no substituents at position 2 thus corresponding to formula **IIa**−**c** is given in Scheme 2. Quinoline-2,5-diones **15a/b**[37,39] were reacted with phosphoryl chloride to give the 2-chloro-substituted quinolin-5-one derivatives **16a/b**, which again offer the introduction of different substituents. In this way, substitution of the chloro group with either alcoholates **18** or amino derivatives **13** yielded **17** (formula **IIa**) and **19** (formula **IIb**) bearing ether or amino linkers, respectively. Alternatively, compound **16** was coupled to ethynyl derivatives **20** in the presence of a palladium(0) catalyst to give additional derivatives of **21**, corresponding to the general formula **IIc**. All substituents R^1 (where R^1 denotes a combination of substituent $R^{1'}$, $R^{1''}$ and a linker group) that were introduced via the above-mentioned procedure are given in Table 2. Introduction of a nitro substituent at R^2 was achieved via nitration of **15b** with nitric acid at 40 °C to give **22** in moderate yields. Thereafter, **22** reacted with phosphoryl chloride leading to **23**, which undergoes substitution reactions with appropriate amino-derivatives **13** to yield a **24a/b** in low to moderate yields. A bromo group was introduced via the same general procedure by bromination of **15b** to give **25**, and subsequent reaction with phosphoryl bromide yielded **26** as shown in Scheme 3.

The substitution of only one bromo group of **26** proceeded in low to moderate yields by application of the appropriate primary or secondary amino derivatives **13** (scheme 3) to give **27a/b**. All substituents R^1 and R^3 introduced via the above-mentioned procedure are shown in Table 3. A HQ with a carboxylic acid group at R^2, **28**, was synthesized starting from **14d** via acid hydrolysis in good yield (80%). The amide **29** was prepared via the coupling reaction of **28** by application of *O*-(benzotriazol-1-yl)-*N*,*N*,*N*′,*N*′-tetramethyluronium tetrafluoroborate (TBTU) as a condensation agent. Compounds **30** and **31** have been synthesized by consecutive substitution of the bromo substituent with the corresponding amines first in position R^1 with 4-(4-fluoro-phenyl)-1,2,3,6-tetrahydro-pyridine and then in position R^2 by applying morpholine. It is worth noticing that the bromo substituent of **30** only bears a low reactivity in comparison with, for example, **25**. Our attempts to carry out a

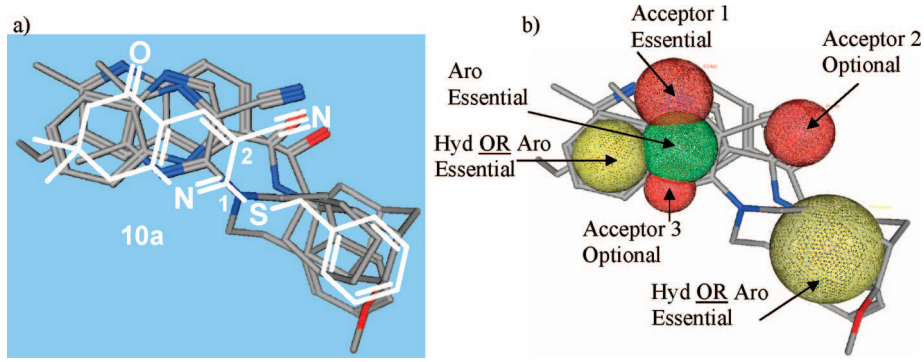

Figure 2. (a) Flexible alignment of known mGluR1 antagonists **1**, **2**, and **3** and (b) allocation of their pharmacophore elements (Acceptor = hydrogen bond acceptor, Hyd = hydrophobic group, Aro = aromatic group).

Scheme 1. Synthesis of 3-cyano-substituted 7,8-dihydro-6H-quinolin-5-ones (R^3 = H, methyl, Hal = Cl, Br, I)

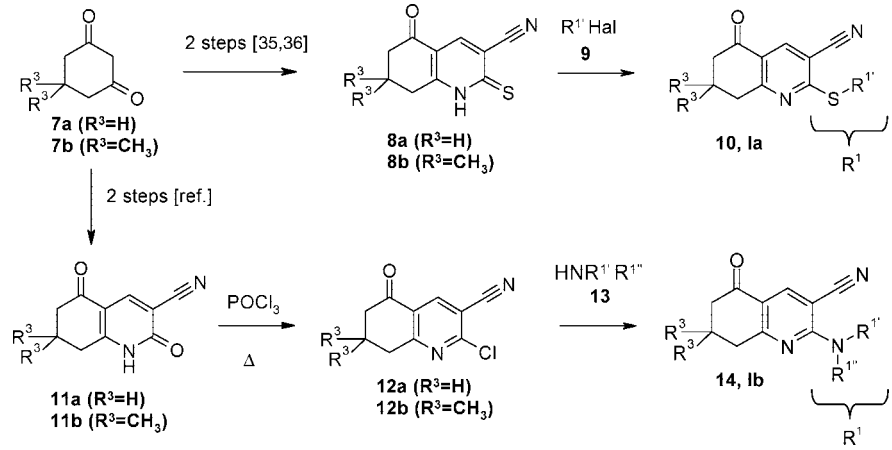

Table 1. Initial HQ Library[a]

	R^1	R^2	R^3	rmGluR1 IC_{50} ± SEM [μM]	rmGluR5 IC_{50} ± SEM [μM]
10a		CN	CH_3	**4.8** ± 1.0	57 ± 22
10b		CN	H	30 ± 18.6	NA
14a		CN	CH_3	2.5 ± 1.6	NA
14b		CN	CH_3	5.3 ± 1.2	NA
14c		CN	H	25 ± 5.7	80 ± 9
17a		H	H	25 ± 7.4	**1.9** ± 0.3
17b		H	CH_3	**21** ± 7.6	12 ± 0.7
19a		H	CH_3	**45** ± 5.0	**8.1** ± 3.0

[a] IC_{50} values were estimated via the simplified logistic equation, where the hill slope is a constant value that equals unity, and the background and the range were also constant values of 0 and 100%, respectively. Real DRC measurements of at least 5 concentrations and 2 independent experiments were plotted in bold: mGluR1 (functional IP3 assay) and mGluR5 (binding). Some of the compounds could not displace [^{3}H]MPEP up to 10 μM and were therefore considered as not active (NA).

Suzuki coupling[40,41] at R^2 of **30** failed and resulted in debromination. Therefore, the Suzuki coupling was performed via the intermediate **25**. A cyclopentylamine moiety was added after application of triflouromethanesulfonate and resulted in **33a** in moderate yields. The tetrazole derivative **33b** was achieved after reacting **14d** with sodium azide in DMF at elevated temperatures.

Discovery of mGluR1 Antagonists. An initial set of HQ derivatives derived from hit compound **10a** was synthesized to prove that the mGluR1 potency found for **10a** was not a singleton (hit enrichment phase). The library contained analogues of **10a** where the linker group of R^1 was varied, whereas for R^2, hydrogen and cyano substituents were chosen. Since selectivity for mGluR1 versus mGluR5 is a key concern in the reduction of potential side effects,[42] all compounds were tested in mGluR1 and mGluR5 assays (Experimental Section). Table 1 shows that the cyano substituent at R^2 was crucial to inhibit mGluR1 activity. This finding was in agreement with our pharmacophore hypothesis of mGluR1, where the *acceptor2* interaction point was present in most reference compounds. The best inhibition of mGluR1 activity was obtained for derivatives **10a**, **14a**, and **14b**. Furthermore, the combination of a cyano group at R^2 and a methyl group at R^3 was favored. On the other hand, the presence of hydrogen instead of the cyano substituent at R^2 enhances the potency for mGluR5, as shown for **17a** and **19a**.

Obviously, the introduction of appropriate substituents at R^2 favors selectivity for mGluR1 versus mGluR5. With consideration of the initial results presented in Table 1, a set of compounds based on an amino linker of R^1 was developed. The amino linker was favored over the thioether or ether linker because it ensures a higher solubility and the possibility of introducing a broader variety of substituents. Changes in the nature of substituents $R^{1'}$ and $R^{1''}$ considerably influenced the potency for mGluR1. Most potent examples include **14d**, **14n**, **14o**, **14q**, and **14r** with IC_{50} values around and below 100 nM (Table 2). In this way, the potency of **14d** in comparison to the initial hit **6** was improved by a factor of about 60.

Table 2. Variation of R^1 to Achieve Selective mGluR1 Antagonists[a]

	R^1	R^2	R^3	rmGluR1 $IC_{50} \pm$ SEM [μM]	rmGluR5 $IC_{50} \pm$ SEM [μM]
14d	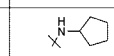	CN	CH_3	**0.078** ± 0.018	49 ± 1.5
14e	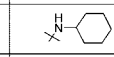	CN	H	3 ± 0.6	NA
14f	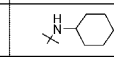	CN	CH_3	4 ± 0.6	NA
14g	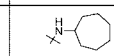	CN	H	7.4 ±	NA
14h	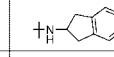	CN	CH_3	1.9 ± 0.3	NA
14i	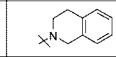	CN	CH_3	1.5 ± 0.3	NA
14j	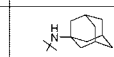	CN	CH_3	41 ± 20.3	NA
14k	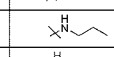	CN	CH_3	2.3 ± 0.5	NA
14l	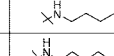	CN	CH_3	1.7 ± 0.3	NA
14m	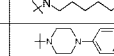	CN	CH_3	2.6 ± 0.5	NA
19b	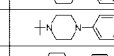	H	H	10.4 ± 2.3	NA
14n	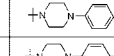	CN	CH_3	**0.13** ± 0.03	NA
14o	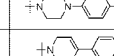	CN	CH_3	**0.16** ± 0.01	NA
14p	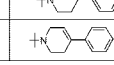	CN	CH_3	7.6 ± 1.1	NA
14q	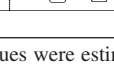	CN	CH_3	< 1.0 ± 0.06	NA
14r	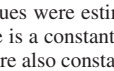	CN	CH_3	**0.11** ± 0.04	NA

[a] IC_{50} values were estimated via the simplified logistic equation, where the hill slope is a constant value that equals unity, and the background and the range were also constant values of 0 and 100%, respectively. Real DRC measurements of at least 5 concentrations were plotted in bold: mGluR1 (functional IP3 assay) and mGluR5 ([^{3}H]-MPEP binding). Some of the compounds could not displace [^{3}H]MPEP up tp 10 μM and were therefore considered as not active (NA).

Scheme 2. Synthesis of 3-Unsubstituted HQs (R^3 = H, methyl, Hal = Cl, Br, I)

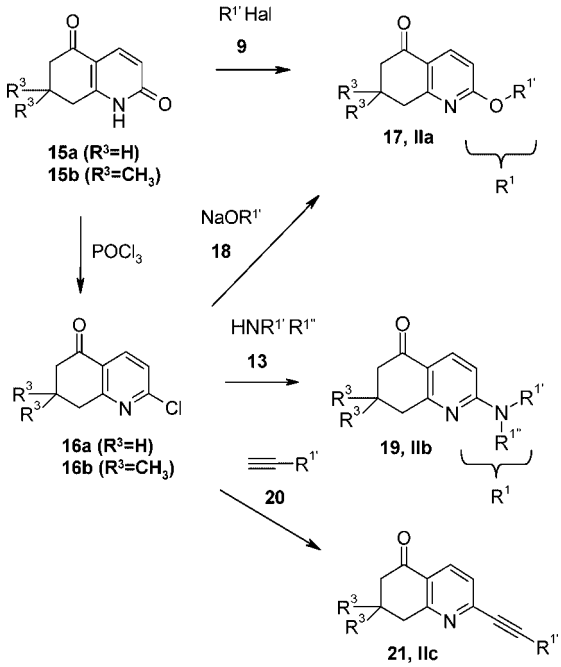

Obviously, small hydrophobic or hydrophobic aromatic substituents of a defined geometry at R^1 were favored to inhibit mGluR1 activity. However, slight structural changes, for example, an increase of the ring size from cyclopentyl (**14d**) to cyclohexyl (**14f**), decreased the potency for mGluR1 by a factor of 50. Apart from cyclopentyl (**14d**), the introduction of tetrahydropiperidyl (**14q**, **14r**) and piperazinyl (**14n**, **14o**) substituents at R^1 resulted in potent mGluR1 antagonists (**14n**, **14o**, **14q** and **14r**). According to Table 2, the presence of substituents within the phenyl ring leads to ambiguous activity results: The piperazinyl derivatives **14n**, bearing no substituent within the phenyl ring, and **14o**, with a fluoro group, both significantly antagonized the mGlu1 receptor within the same order of magnitude, whereas the presence of a methoxyl substituent in **14p** was followed by a considerable decrease of the potency. In contrast, tetrahydropiperidyl derivative **14r**, carrying a fluoro group, was found to be more potent than the nonsubstituted analogue **14q**. The same trend holds true for the influence of the methyl substituent at R^3 that was also less obvious: In some cases an up to 5-fold increase of the antagonistic effect was found (**10a** vs **10b**), whereas in other cases, no impact on the functional mGluR1 activity was observed (**14 e**, **14f**).

Table 3. Variation of R^2 to achieve selective mGluR1 antagonists[a]

	R^1	R^2	rmGluR1 $IC_{50} \pm$ SEM [μM]	rmGluR5 $IC_{50} \pm$ SEM [μM]
14d		CN	**0.078** ± 0.018	49 ± 1.5
27c		Cl	7.9 ± 1.3	3.5 ± 0.1
27a		Br	NA	29 ± 1
28		COOH	23 ± 7.1	NA
29		C(=O)NMe2	21 ± 1.7	58 ± 4
33a			NA	NA
33b			13 ± 2.5	NA
24b		NO_2	12 ±3	NA
27b		Br	≤1[b]	37 ± 3
31			15 ± 3	NA

[a] IC_{50} values were estimated via the simplified logistic equation, where the hill slope is a constant value that equals unity, and the background and the range were also constant values of 0 and 100%, respectively: mGluR1 (functional FLIPR assay except **27b**) and mGluR5 (binding). Some of the compounds could not displace [^{3}H]MPEP up to 10 μM and were therefore considered as not active (NA). [b] No DRC because of solubility problems.

A broader variation of R^2 according to Scheme 3 is listed in Table 3. The best results were obtained after the introduction of a bromo (**27b**) or chloro (**27c**) substituent. However, here, the mGluR1 activity was considerably influenced by the combination of the substituent R1 and R2 (e.g., **27a**, **27b**). Overall, among all substituents that were tested and listed in Table 3, no alternative for the cyano group could be identified. Unfortunately, the presence of a dimethylamido (**29**) or a carboxylic acid group (**28**), which resulted in a considerable improvement in solubility, gave a significant reduction of potency. Heterocyclic groups such as pyrimidino or tetrazol substituents also decreased or abolished potency for mGluR1.

Discovery of mGluR5 Antagonists and Positive Allosteric Modulators. All compounds that were prepared according to Scheme 2 were screened in a mGluR5 binding assay as mentioned above, as well as in a functional assay detecting changes in the calcium level (for details see Supporting Information). Such compounds bearing an ethynyl linker (**21**,

Scheme 3. Introduction of Substituents at Position R^2

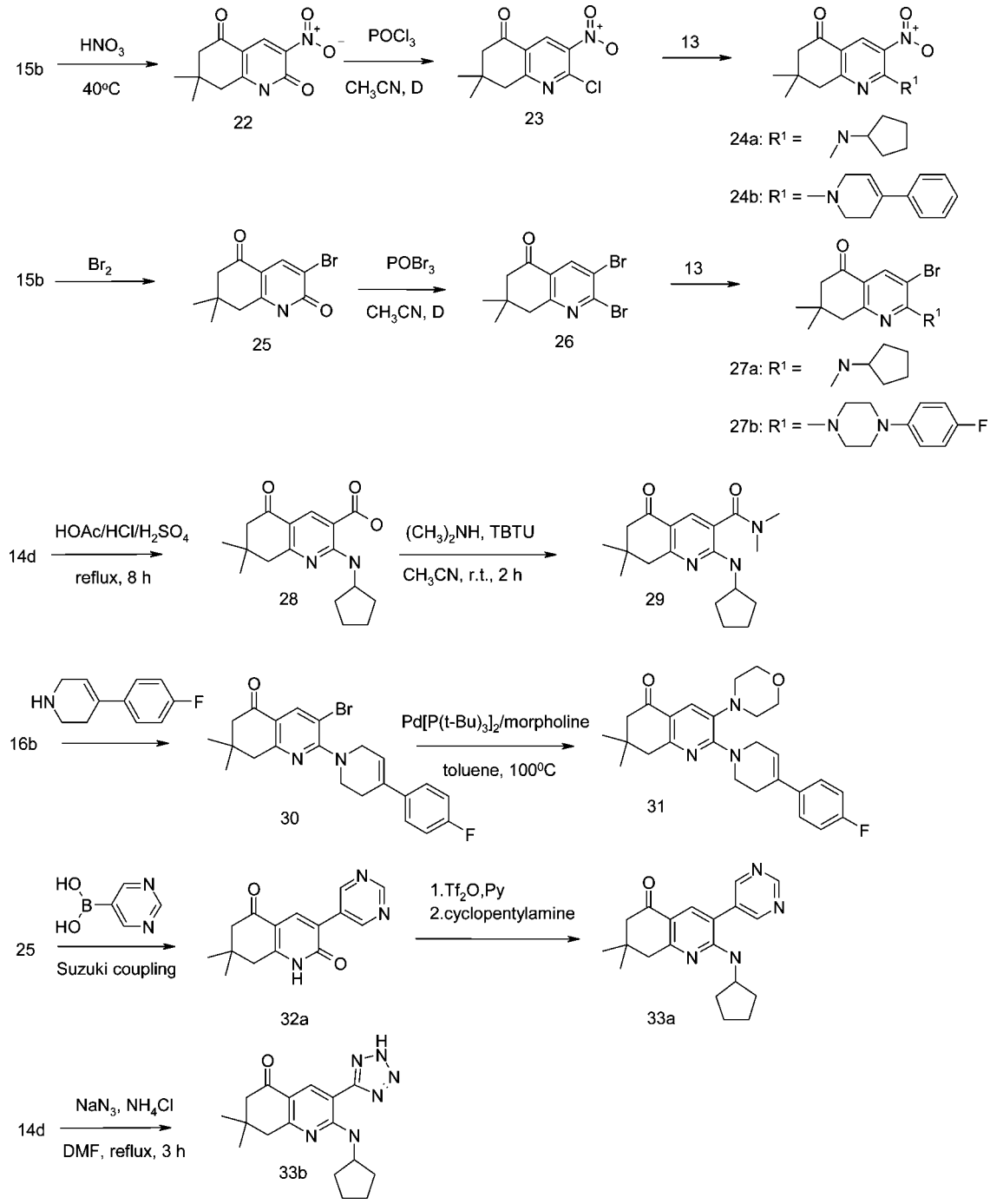

IIc) were found to interact with the mGluR5 receptor. This observation was somewhat expected because derivatives of **IIc** show a high structural similarity with the known mGluR5 antagonist MPEP[43] (Table 4). In a binding assay, **21a** moderately displaced [^{3}H]MPEP with an affinity of 800 nM. However, in a functional assay, **21a** did not behave like MPEP: instead of acting as an inhibitor, **21a** potentiated the calcium signals. Functional activation of mGluR5 by orthosteric ligands (agonists as L-quisqualate or L-glutamate) was measured in fluorescent imaging plate reader (FLIPR) assays as transient increases of intracellular calcium signals. In such a FLIPR assay with rat astrocytes mGluR5 was selectively activated by L-quisqualate. Here, a considerable and dose-dependent potentiation of a low calcium signal, elicited by a 10 nM L-quisqualate (open triangle in Figure 3a), was observed when **21a** was preincubated prior to agonist stimulation. The EC_{50} of this potentiation was 0.034 $\pm$ 0.009 μM, and **21a** gave no calcium signals (open circles).

When tested on agonist (L-quisqualate) concentration–response curves, the addition of a fixed concentration (10 μM) of **21a** lead to a 2.0-fold left shift, corresponding to an increase in agonist potency (EC_{50}) from 24 $\pm$ 1.9 to 12 $\pm$ 1.7 nM (Figure 3b). This behavior was even more pronounced for the human mGluR5 receptor, where the native agonist L-glutamate was applied (Figure 3c). Here, a 3.2-fold left shift was obtained corresponding to a change of the L-glutamate EC_{50} from 0.77 $\pm$ 0.07 to 0.24 $\pm$ 0.05 μM.

Because of the high structural similarity of **21a** with the known antagonist MPEP[43] (Table 4), we were wondering whether the positive modulation was achieved via the presence of the carbonyl group of **21a**, enabling **21a** to form an additional

Table 4. Potencies and Potentiation Properties of Positive Modulators of mGluR5 Measured via Calcium Signal[a]

	IC_{50} (μM) rmGluR5	Ki (μM) rmGluR5	EC_{50} (μM) rmGluR5 (hmGluR5)	-fold potentiation rmGluR5 (hmGluR5)
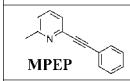 **MPEP**	**0.013 ± 0.001**	0.012 ±0.002	-	-
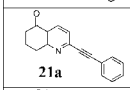 **21a**	-	**0.8 ± 0.1**	**0.034 ± 0.009** (0.172 ± 0.049)	2.0 ± 0.1 (3.5 ± 0.6)
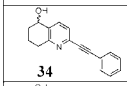 **34**	-	7.6 ± 0.1	**0.49 ± 0.06** (1.13 ± 0.11)	2.2 ± 0.5 (2.0)
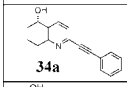 **34a**	-	**9.28 ± 0.9**	0.25 ± 0.1 (1.08 ± 0.11)	2.0 ± 0.4 (2.5 ± 0.3)
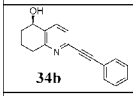 **34b**	-	**4.71 ± 0.2**	0.18 ± 0.2 (0.98 ± 0.13)	3.1 ± 0.4 (2.5± 0.4)
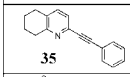 **35**	**0.51 ± 0.08**	**1.5** ± 0.2	-	-
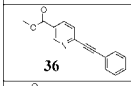 **36**	4.6 ± 1.7	**1.4** ± 0.3	-	-
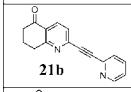 **21b**	60 ± 11	2.36 ± 0.01	-	-
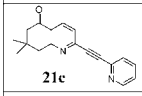 **21c**	**2.6 ± 1.6**	0.21 ± 0.03	-	-
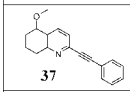 **37**	**0.08 ± 0.008**	**0.139 ± 0.007**	-	-
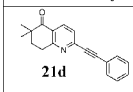 **21d**	**0.023 ± 0.005**	**0.051 ± 0.002**	-	-

[a] Antagonists of mGluR5 displacing [^{3}H]MPEP in a binding assay.

hydrogen bond. Therefore, several derivatives of **21a** were synthesized according to Scheme 2: the most interesting examples were listed in Table 4. A positive modulation was achieved only for those compounds bearing a carbonyl or a hydroxyl group at the unsaturated ring and two hydrogen substituents at R^3. However, even though the EC_{50} value of **34**, bearing a hydroxyl group, was considerably higher (0.49 μM), its maximal change of quisqualate EC_{50} was found practically unchanged in comparison to that of **21a.** A separation of the enantiomers of **34**, **34a**, and **34b** was achieved by application of chiral column chromatography. For both enantiomers, similar activity and potentiation, compared to that of the racemic compound **34**, were observed.

In case where the carbonyl group was removed (**35**), a significant negative modulation was achieved with an IC_{50} of 500 nM. Furthermore, the orientation of the carbonyl group seems to be crucial because the open analogue **36** again showed a moderate antagonistic effect. Therefore, it seems that the presence of a hydrogen-bond acceptor at a fixed position facilitates positive modulation within the transmembrane domain. The etherification of **34** yielded the methyl ether derivative **37**, which was found to be a potent mGluR5 antagonist with an IC_{50} value of about 80 nM. Interestingly, even small structural changes, such as the introduction of two methyl-substituents at R^3 (**21c**), abolished the ability to induce a positive modulation of mGluR5, and only a moderately active mGluR5 antagonist was obtained. The exchange of the phenyl ring of **21a** by a pyridyl ring in **21b** gave only a mGluR5 antagonist of weak potency. However, a slight variation

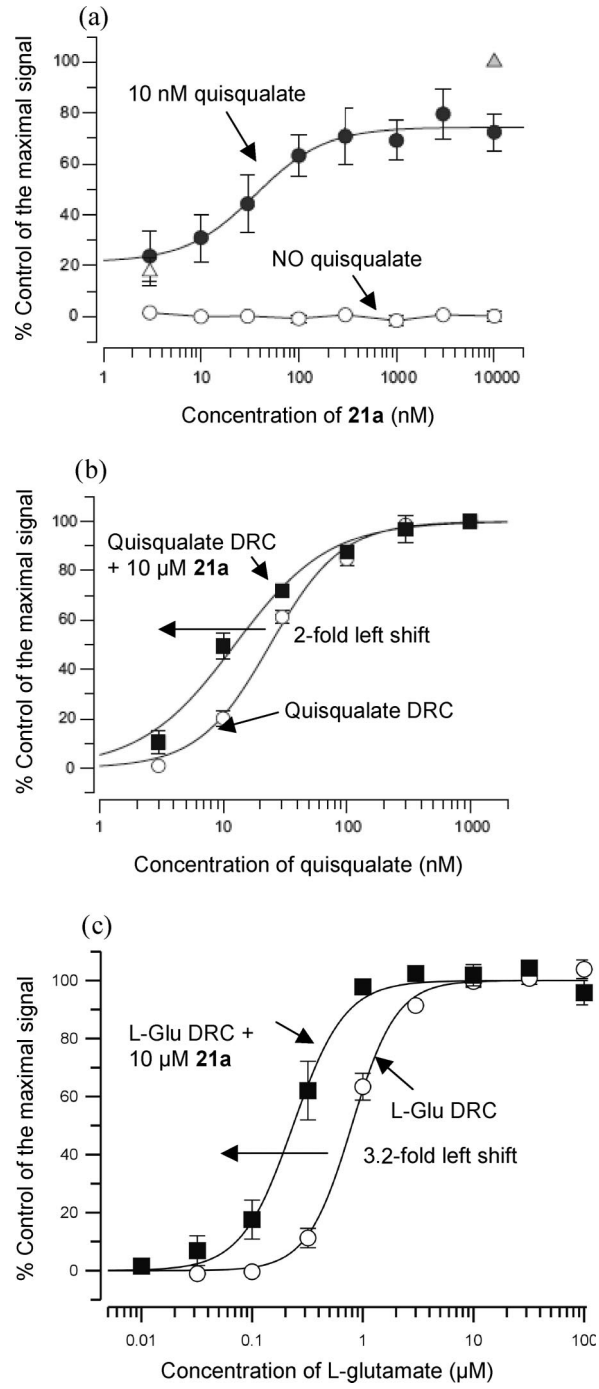

Figure 3. (a) Calcium signals of mGluR5 (rat) in dependence of concentrations of **21a** before (open circles) and after (filled circles) stimulation with 10 nM L-quisqualate. Ten (open triangle) and 100 nM (gray triangle) L-quisqualate signals were depicted as controls. (b) Concentration–response curves of quisqualate without (circles) and with (squares) after preincubation of 10 μM **21a** at mGluR5 (rat). (c) Concentration–response curves of L-glutamate with (squares) and without (circles) 10 μM **21a** at mGluR5 (human). Averaged from at least 3 independent experiments that were performed in quadruplicate.

of the position of the dimethyl groups yielded the highly potent mGluR5 antagonist **21d** with an IC_{50} of 20 nM. These results show that, in analogy to negative modulators of mGluR1 that have been described before, minor structural changes could have a strong impact in the functional profile of mGluR5 and that the interpretation of the structure–activity relationship is therefore rather challenginag.[44]

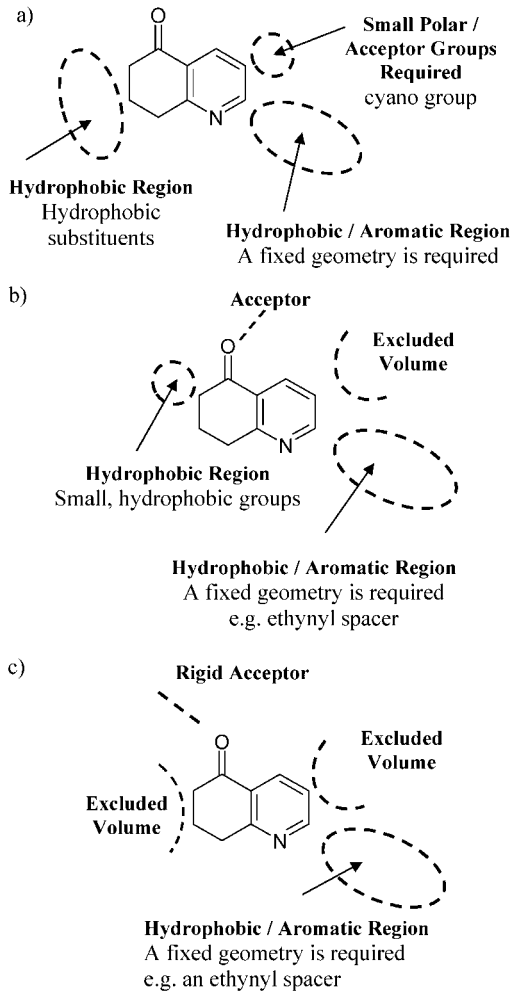

Figure 4. (a) Essential functionalities for mGluR1 antagonists, (b) mGluR5 antagonists, and (c) mGluR5 positive modulators based on a HQ scaffold.

Figure 4 summarizes the essential pharmacophore elements based on the structure–activity relationship information from Tables 1−4. At R^1, a hydrophobic or hydrophobic/aromatic substituent with a fixed geometry is one of the main elements to achieve potency for mGluR1 (Figure 4a). To obtain potent and subtype-selective mGluR1 antagonists, a small acceptor group at R^2, ideally a cyano group, seems to be essential. Within the saturated ring close to the carbonyl group, the presence of hydrophobic substituents is beneficial. To achieve mGluR5 antagonistic activity, an ethynyl spacer at R^1, no substituents at R^2, and small, hydrophobic substituents close to the carbonyl group are required.

In contrast, mGluR5 positive modulators based on a HQ scaffold are characterized by the absence of functional groups at the unsaturated HQ ring, in addition to the presence of an acceptor group (e.g., carbonyl or hydroxyl group) in the HQ ring, which could form hydrogen bonds with the TM helices.

Visualization of the Binding Cleft. To gain an improved understanding of the SAR information, ligand **14q** was selected for a further analysis of the binding mode of the HQ scaffold because of the combination of activity on mGluR1, selectivity versus mGluR5, the presence of one of the most voluminous R^1 groups, and the structural high similarity with more complex and potent derivatives (e.g., **19b**, **14r**). A detailed description of the construction of a homology model of mGluR1 is given in the Supporting Information. Compound **14q** was placed manually in the transmembrane region in proximity to the pocket where 11-*cis*-retinal was found in bovine rhodopsin[26] and cominimized with the receptor. The binding mode of **14q** was selected according to the observed SAR (Figure 5, see text below). The calculated conformation of **14q** in the receptor reveals an internal energy near the global minimum obtained from conformational analysis (80.281 vs 80.249 kcal/mol). According to our homology model, the key interactions of the pharmacophore for mGluR1 (Figure 2b) were hydrogen-bonding interactions with residues R661 (3.29) for acceptor 1, T815 (7.39) for acceptor 2, and S668 (3.36) for acceptor 3. The hydrophobic and aromatic features were placed close to W798 (6.48), V664 (3.32), and L640 (2.58). The carbonyl-oxygen of the unsaturated ring of HQ potentially interacts as hydrogen-bond acceptor 1 with a hydrogen-bonding network of R661 (3.29), N747 (45.51), and backbone atoms of EL2. This arginine (which is conserved in mGluR5) has also been shown to affect binding of the mGluR5 allosteric negative modulator MPEP (Table 4).[45] N750A (45.54) increased the effect of the mGluR1 negative allosteric modulator EM-TBPC (Figure 1)[46] and might thus be assumed to be in contact with the ligand, as found in our proposed binding mode for **14q**. The cyano group of **14q** (acceptor 2) could interact with T815 (7.39) that has been shown previously to be involved in the binding of the mGluR1 negative allosteric modulator EM-TBPC (Figure 1).[46] The selectivity for mGluR1 over mGluR5 for such molecules containing the cyano group compared with molecules with hydrogen at R^2 agrees well with the model: At position 7.39, T815 was found in mGluR1, whereas at position 7.39 in mGluR5, methionine was present in mGluR5. This change from a small hydrophilic (mGluR1) to a larger and more hydrophobic side chain in mGluR5 might lead to a steric hindrance and thus repulsion of the cyano group of these HQs in the mGluR5 binding site. The third hydrogen-bonding interaction (acceptor 3) could be formed via the aromatic acceptor nitrogen and S668 (3.36). Previously, position 3.36 has been shown to be involved in the binding of MPEP in mGluR5.[45] We felt confident to assume a potential interaction of mGluR1 modulators with residues that were involved in the binding of mGluR5 modulators because the binding site of mGluR1 is known to partially overlap with the TM mGluR5 pocket.[28] The two methyl groups of the R^3 position interact with a hydrophobic cluster of TM3 residues V753 (5.43), P756 (5.46), and V757 (5.47).

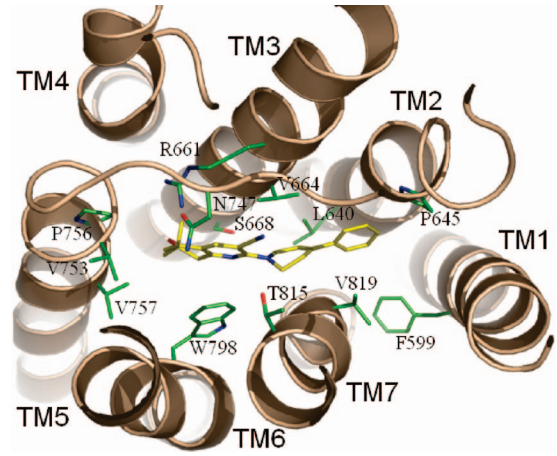

Figure 5. Putative binding mode of **14q** inside the allosteric binding site of mGluR1.

The preference of nonaromatic over aromatic ring systems at R^1 in close proximity to the HQ scaffold agrees well with a

close interaction of this ring with V664 (3.32), as predicted by the model. V664 might also be involved in the observed selectivity of **14q** for mGluR1. In GluR5, isoleucine was found at position 3.32, which results in a decrease in the accessible volume. The presence of the relatively large isoleucine group might also explain the preference for mGluR5 antagonists bearing an ethynyl linker at R^1, which was found in positive and negative HQ modulators of mGluR5. The distant aromatic ring at R^1 could interact with a hydrophobic cluster of L640 (2.58), P645 (2.63), V819 (7.43), and potentially, F599 (1.42).

The predicted binding pocket of **14q** seems to overlap with the binding pocket of the mGluR1 negative allosteric inhibitor EM-TBPC (Figure 1), for which residues influencing the binding of the ligand have been determined experimentally by mutational analysis.[46] V757 (5.47), W798 (6.48), F801 (6.51), Y805 (6.55), and T815 (7.39) were found to affect EM-TBPC binding when mutated to the respective mGluR5 residues. All of these residues were found close to the putative binding site of **14q**. However **14q** exceeds the binding pocket of EM-TBPC, and it might form additional interactions with, for example, TM2 and TM1. The putative binding mode for **14q** is in agreement with our SAR and published mutational data from other ligands and might thus provide a further starting point for the design and optimization of other mGluR1 modulators. In addition, these investigations might pave the way toward a better understanding of the ligand–receptor interactions in class C GPCRs.

Conclusion

We have presented the development of a pharmacophore model for allosteric mGluR1 antagonists based on published mGluR1 reference ligands. This model was applied successfully to screen a diverse compound library, and it facilitated the identification of mGluR1 antagonists with low micromolar affinity with a hit rate of about 10%. Compound **10a** was chosen for a hit optimization program because of its novelty, as well as the suitability of its scaffold for a parallel synthesis approach. A focused library of HQ derivatives led to the discovery of highly potent mGluR1 and mGluR5 antagonists, as well as potent mGluR5 positive modulators. The presence of both positive and negative modulators of mGluR1 and mGluR5 based on the same HQ scaffold was mainly attributed to the fact that these receptors have similar "overlapping" allosteric binding sites. Furthermore, it turned out that minor structural changes at distinct positions of the HQ scaffold could have a considerable impact on their potency and selectivity profile. Our results show that a novel scaffold interacting within this binding side could be fine-tuned toward positive and negative modulation of mGluR1 and mGluR5. The approach described herein could, in principle, be applied for the identification of other mGluR modulators where only little or no ligand information is available.

Experimental Section

(A) Chemistry. (The synthesis of all intermediate compounds is given in the Supporting Information.)

General Information. The solvents used were of commercial grade; tetrahydrofuran (THF) was dried over potassium, and toluene was distilled from sodium. ^{1}H and ^{13}C NMR spectra were recorded on a Bruker DRX 500 (500 and 125 MHz, respectively), Bruker AMX 300 (300 and 75 MHz, respectively), or Varian MERCURY (400 MHz) spectrometer. Melting points were taken on a Sanyo Gallenkamp melting point apparatus (MPD350.BM3.5) and were uncorrected. The LC/MS analyses for the compounds were done at Surveyor MSQ (Thermo Finnigan, U.S.A.) with APCI ionization. Tetrakis(triphenylphosphine)-palladium(0) ($Pd(PPh_3)_4$) and dichloro[1,1′-bis(diphenylphosphino)ferrocene]palladium(II) dichloromethane adduct ($Pd(dppf)_2Cl_2$ catalysts were purchased from ABCR, and bis-(ditertbutylphosphine)-palladium(0) was purchased from Strem Chemicals, Inc. The purity of all compounds was determined via HPLC column chromatography (Shimadzu LC-20Aprominence; compound dissolved in acetonitrile/water 50/50 with 0.5% DMSO; column Phemomenex Gemini 50 × 4.6 mm, 3 μM; mobile phase acetonitrile/water with 0.1% formic acid; flow 2 mL/min; detection UV at 310 nm, ambient temperature). The synthesis of several HQ derivatives has been described in a patent application.[47,48]

2-Benzylsulfanyl-7,7-dimethyl-5-oxo-5,6,7,8-tetrahydroquinoline-3-carbonitrile (10a). To a solution of 7,7-dimethyl-5-oxo-2-thioxo-1,2,5,6,7,8-hexahydroquinoline-3-carbonitrile (0.5 g, 2.2 mmol) in DMF (4 mL) was added 10% aqueous KOH (1.23 mL), followed by dropwise addition of benzyl bromide (0.25 mL, 2.2 mmol). The mixture was stirred at room temperature for 12 h; then water (12 mL) was added. The precipitate formed within 2 h was filtered off, washed with water, and recrystallized from hexane/ethyl acetate mixture. A yellow solid was obtained (0.61 g, 86%) with mp = 129–130 °C. ^{1}H NMR ($CDCl_3$, TMS): δ 1.13 (s, 6H), 2.54 (s, 2H), 3.05 (s, 2H), 4.55 (s, 2H), 7.3–7.4 (m, 5H), 8.32 ppm (s, 1H). MS: *m/z* ($APCI^+$) 323 ($M + H^+$). Purity (HPLC): 97.89%.

2-Benzylsulfanyl-5-oxo-5,6,7,8-tetrahydroquinoline-3-carbonitrile (10b). To a solution of 5-oxo-2-thioxo-1,2,5,6,7,8-hexahydroquinoline-3-carbonitrile (0.45 g, 2.2 mmol) in DMF (4 mL) was added 10% aqueous potassium hydroxide (1.23 mL), followed by dropwise addition of benzyl bromide (0.25 mL, 2.2 mmol). The mixture was stirred at room temperature for 12 h; then water (12 mL) was added. The product was extracted with diethyl ether. The extract was washed with water and dried over sodium sulfate. Filtration and concentration under reduced pressure afforded a residue that was purified by flash chromatography on silica gel (petroleum ether/ethyl acetate, 10:1) to give the title compound in a 91% yield as a colorless solid with mp = 137–138 °C. ^{1}H NMR ($CDCl_3$, TMS): δ 2.20 (m, 2H), 2.69 (t, 6 Hz, 2H), 3.16 (t, 6 Hz, 2H), 4.54 (s, 2H), 7.3−7.4 (m, 5H); 8.33 (s, 1H). MS: *m/z* ($APCI^+$) 295 ($M + H^+$). Purity (HPLC): 97.89%.

2-Benzylamino-7,7-dimethyl-5-oxo-5,6,7,8-tetrahydroquinoline-3-carbonitrile (14a). A solution of 7,7-dimethyl-2-methylsulfanyl-5-oxo-5,6,7,8-tetrahydroquinoline-3-carbonitrile (0.25 g, 1 mmol), benzylamine (0.13 g, 1.2 mmol), and sodium acetate (0.41 g, 3 mmol) in dry ethanol (3 mL) was stirred while boiling at reflux for 60 h. The reaction mixture was then evaporated under reduced pressure. The residue was purified by flash chromatography on silica gel (chloroform/methanol, 30:1) and treated with dry HCl solution in diethyl ether to give the title compound (0.072 g, 21%) as a colorless solid with mp = 163–164 °C. ^{1}H NMR ($CDCl_3$, TMS): δ 1.11 (s, 6H), 2.48 (s, 2H), 2.95 (s, 2H), 4.88 (d, 4.2 Hz, 2H), 7.38 (m, 5H), 8.38 (s, 1H). Purity (HPLC): 100%.

2-(Benzyl-methyl-amino)-7,7-dimethyl-5-oxo-5,6,7,8-tetrahydroquinoline-3-carbonitrile (14b). Compound **12b** (0.220 g, 0.94 mmol), *N*-methyl-benzylamine (1.70 g, 1.40 mmol), and triethylamine (0.10 g, 1.0 mmol) in ethanol (3 mL) were refluxed for 5 h (TLC control, chloroform/hexane, 2:1). Then, the mixture was diluted with water (20 mL) and extracted with dichloromethane (2 × 10 mL). The combined extracts were concentrated, and the residue was separated by column chromatography on silica gel (dichloromethane/hexane, 1:1). The subsequent recrystallization from ethanol resulted in 0.145 g (48%) of pure compound **14b** (mp = 97–99 °C). ^{1}H NMR (DMSO-d_6, 400 MHz): δ_H 1.01 (s, 6H), 2.43 (s, 2H), 2.80 (s, 2H), 3.33 (s, 3H), 5.05 (s, 2H), 7.24–7.38 (m, 5H), 8.21 (s, 1H). MS: *m/z* ($APCI^+$) 320 ($M + H^+$). Purity (HPLC): 99.55%.

2-(Benzyl-methyl-amino)-5-oxo-5,6,7,8-tetrahydroquinoline-3-carbonitrile (14c). Compound **12a** (0.154 g, 0.75 mmol), *N*-methyl-benzylamine (1.82 g, 1.50 mmol), and triethylamine (0.083 g, 0.82 mmol) in ethanol (3 mL) were refluxed for 5 h (TLC control, chloroform/hexane, 2:1). Then, the mixture was diluted with water (10 mL). The precipitate was filtered off and recrystallized from ethanol to give 0.085 g (39%) of compound **14c** (mp = 103–105 °C). ^{1}H NMR (DMSO-d_6, 400 MHz): δ_H 1.95–2.08 (s, 2H), 2.48–2.58 (m, 2H), 2.87 (t, J = 7 Hz, 2H), 3.33 (s, 3H), 5.05

(s, 2H), 7.23–7.38 (m, 5H), 8.21 (s, 1H). MS: *m/z* ($APCI^+$) 292 ($M + H^+$). Purity (HPLC): 98.64%.

2-Cyclopentylamino-7,7-dimethyl-5-oxo-5,6,7,8-tetrahydroquinoline-3-carbonitrile (14d). Compound **14d** was synthesized from **12b** and cyclopentylamine, using the procedure described for **14b**, as a white solid (mp = 154–156 °C, yield = 80%). ^1H NMR (DMSO-d_6, 400 MHz): δ_H 1.00 (s, 6H), 1.47–1.82 (m, 6H), 1.85–2.05 (m, 2H), 2.43 (s, 2H), 2.80 (s, 2H), 4.43–4.56 (m, 1H), 7.54 (br. s, 1H), 8.14 (s, 1H). MS: *m/z* ($APCI^+$) 284 ($M + H^+$). Purity (HPLC): 98.39%.

2-Cyclohexylamino-5-oxo-5,6,7,8-tetrahydroquinoline-3-carbonitrile (14e). Compound **14e** was synthesized from **12a** and cyclohexylamine, using the procedure described for **14c**, as a white solid (mp = 143–145 °C, yield = 59%). ^1H NMR (DMSO-d_6, 400 MHz): δ_H 1.00 (s, 6H), 1.00–1.90 (m, 10H), 2.40 (s, 2H), 2.80 (s, 2H), 4.01–4.15 (m, 1H), 7.41 (br. s, 1H), 8.14 (s, 1H). MS: *m/z* ($APCI^+$) 270 ($M + H^+$). Purity (HPLC): 99.80%.

2-Cyclohexylamino-7,7-dimethyl-5-oxo-5,6,7,8-tetrahydroquinoline-3-carbonitrile (14f). Compound **12b**(0.236 g, 1 mmol), cyclohexylamine (0.120 g, 1.2 mmol), and triethylamine (0.165 mL, 1.2 mmol) were dissolved in acetonitrile (5 mL). The mixture was refluxed for 6 h, and the reaction was monitored by TLC (ethyl acetate/hexane, 1:4). When the reaction was over, the mixture was diluted with 10 mL of water. The formed sediment was filtered off and crystallized from ethanol. As a result, 0.170 g (57%) of compound **14f** was obtained (mp = 164–167 °C). ^1H NMR (DMSO-d_6, 400 MHz): δ_H 1.03–1.20 (m, 2H), 1.20–1.50 (m, 5H), 1.55–1.66 (m, 1H), 1.68–1.78 (m, 2H), 1.78–1.88 (m, 2H), 1.95–2.05 (m, 2H), 2.78–2.95 (m, 2H), 4.02–4.18 (m, 1H), 7.36 (br. s, 1H), 8.16 (s, 1H). MS: *m/z* ($APCI^+$) 298 ($M + H^+$). Purity (HPLC): 98.34%.

2-Azepanyl-5-oxo-5,6,7,8-tetrahydroquinoline-3-carbonitrile (14g). Compound **14g** was synthesized from **12a** and azepane, using the procedure described for **14c**, as a white solid (mp = 76–78 °C, yield = 38%). ^1H NMR (DMSO-d_6, 400 MHz): δ_H 1.46–1.58 (m, 4H), 1.74–1.87 (m, 4H), 1.95–2.07 (m, 2H), 2.48–2.58 (m, 2H), 2.82–2.92 (m, 2H), 3.85–3.97 (m, 4H), 8.17 (s, 1H). MS: *m/z* ($APCI^+$) 270 ($M + H^+$). Purity (HPLC): 99.60%.

2-(Indan-2-ylamino)-7,7-dimethyl-5-oxo-5,6,7,8-tetrahydroquinoline-3-carbonitrile (14h). Compound **12b** (0.236 g, 1 mmol), indane-2-yl-amine (0.160 g, 1.2 mmol), and triethylamine (0.165 mL, 1.2 mmol) were dissolved in 5 mL of ethanol. The mixture was refluxed for 6 h, and the reaction was monitored by TLC (ethyl acetate/hexane, 1:4). When the reaction was over, the mixture was diluted with 10 mL of water. The formed sediment was filtered off, washed with water, and crystallized from ethanol. As a result, 0.175 g (53%) of compound **14h** was obtained as a white solid (mp = 184–186 °C). ^1H NMR (DMSO-d_6, 400 MHz): δ_H 1.03 (s, 6H), 2.43 (s, 2H), 2.82 (s, 2H), 2.96–3.15 (m, 2H), 3.17–3.35 (m, 2H), 4.90–5.05 (m, 1H), 7.14 (br. s, 2H), 7.24 (br. s, 2H), 7.93 (br. s, 1H), 8.19 (s, 1H).MS: *m/z* ($APCI^+$) 332 ($M + H^+$). Purity (HPLC): 99.00%.

2-(3,4-Dihydro-1H-isoquinolin-2-yl)-7,7-dimethyl-5-oxo-5,6,7,8-tetrahydroquinoline-3-carbonitrile (14i). Compound **12b** (0.236 g, 1 mmol), 1,2,3,4-tetrahydroisoquinoline (0.16 g, 1.2 mmol), and triethylamine (0.165 mL, 1.2 mmol) were dissolved in 5 mL of acetonitrile. The mixture was refluxed for 6 h, and the reaction was monitored by TLC (ethyl acetate/hexane, 1:4). When the reaction was over, the mixture was diluted with water (10 mL). The formed sediment was filtered off and crystallized from ethanol. As a result, 0.200 g (60%) of compound **14i** was obtained (mp = 132–134 °C). ^1H NMR (DMSO-d_6, 400 MHz): δ_H 1.02 (s, 6H), 2.46 (s, 2H), 2.87 (s, 2H), 3.03 (t, J = 7 Hz, 2H), 4.08 (t, J = 7 Hz, 2H), 4.7 (s, 2H), 7.17–7.29 (br. s, 4H), 8.28 (s, 1H). MS: *m/z* ($APCI^+$) 332 ($M + H^+$).

2-(Adamantan-1-ylamino)-7,7-dimethyl-5-oxo-5,6,7,8-tetrahydroquinoline-3-carbonitrile (14j). Compound **12b** (0.236 g, 1 mmol), adamantanylamine (0.450 g, 2 mmol), and triethylamine (0.28 mL, 2 mmol) were dissolved in 5 mL of ethanol, and the mixture was refluxed for 24 h. The reaction was monitored by TLC (ethyl acetate/hexane, 1:4). Then, the mixture was cooled. The formed sediment was filtered off, washed with water, and crystallized with ethanol. As a result, 0.04 g (11%) of compound **14j** was obtained as a white solid (mp = 266–268 °C). ^1H NMR (DMSO-d_6, 400 MHz): δ_H 1.02 (s, 6H), 1.68 (s, 6H), 2.09 (s, 3H), 2.20 (s, 6H), 2.43 (s, 2H), 2.84 (s, 2H), 6.20 (br. s, 1H), 8.16 (s, 1H).MS: *m/z* ($APCI^+$) 350 ($M + H^+$). Purity (HPLC): 97.59%.

7,7-Dimethyl-5-oxo-2-propylamino-5,6,7,8-tetrahydroquinoline-3-carbonitrile (14k). Compound **14k** was synthesized from **12b** and propylamine, using the same procedure as described for **14b**, as a white solid (mp = 122–125 °C, yield = 43%). ^1H NMR (DMSO-d_6, 400 MHz): δ_H 0.88 (t, J = 7 Hz, 3H), 1.00 (s, 6H), 1.53–1.67 (m, 2H), 2.41 (s, 2H), 2.80 (s, 2H), 3.42 (m, 2H), 7.83 (br. s, 1H), 8.15 (s, 1H).MS: *m/z* ($APCI^+$) 258 ($M + H^+$). Purity (HPLC): 98.10%.

2-Butylamino-7,7-dimethyl-5-oxo-5,6,7,8-tetrahydroquinoline-3-carbonitrile (14l). Compound **14l** was synthesized from **12b** and butylamine, using the same procedure described for **14b**, as a white solid (mp = 107–110 °C, yield = 41%). ^1H NMR (DMSO-d_6, 400 MHz): δ_H 0.92 (t, J = 7 Hz, 3H), 1.02 (s, 6H), 1.25–1.43 (m, 2H), 1.44–1.65 (m, 2H), 2.41 (s, 2H), 2.80 (s, 2H), 3.46 (m, 2H), 7.88 (t, J = 7 Hz, 1H), 8.16 (s, 1H). MS: *m/z* ($APCI^+$) 272 ($M + H^+$). Purity (HPLC): 98.52%.

2-Hexylamino-7,7-dimethyl-5-oxo-5,6,7,8-tetrahydroquinoline-3-carbonitrile (14m). Compound **14m** was synthesized from **12b** and hexylamine, using the same procedure described for **14b**, as a white solid (mp = 88–89 °C, yield = 30%). ^1H NMR (DMSO-d_6, 400 MHz): δ_H 0.80–0.93 (m, 3H), 1.00 (s, 6H), 1.20–1.35 (m, 6H), 1.49–1.65 (m, 2H), 2.40 (s, 2H), 2.78 (s, 2H), 3.38–3.52 (m, 2H), 7.78 (br. s, 1H), 8.14 (s, 1H). MS: *m/z* ($APCI^+$) 300 ($M+H^+$). Purity (HPLC): 99.97%.

7,7-Dimethyl-5-oxo-2-(4-phenyl-piperazin-1-yl)-5,6,7,8-tetrahydroquinoline-3-carbonitrile (14n). Compound **14n** was synthesized from **12b** and 4-phenylpiperazine, using the procedure described for **14b**, as a white solid (mp = 167–170 °C, yield = 62%). ^1H NMR (DMSO-d_6, 400 MHz): δ_H 1.02 (s, 6H), 2.47 (s, 2H), 2.84 (s, 2H), 3.32 (br. s, 4H), 4.05 (br. s, 4H), 6.80 (t, J = 7 Hz, 1H), 6.97 (d, J = 7 Hz, 2H), 7.23 (t, J = 7 Hz, 2H), 8.28 (s, 1H). MS: *m/z* ($APCI^+$) 361 ($M + H^+$). Purity (HPLC): 99.18%.

2-[4-(4-Fluoro-phenyl)-piperazin-1-yl]-7,7-dimethyl-5-oxo-5,6,7,8-tetrahydroquinoline-3-carbonitrile (14o). Compound **12b** (0.236 g, 1 mmol), 4-fluoro-phenyl-piperazine (0.216 g, 1.2 mmol), and triethylamine (0.165 mL, 1.2 mmol) were dissolved in 5 mL of acetonitrile. The mixture was refluxed for 6 h, and the reaction was monitored by TLC (ethyl acetate/hexane, 1:4). When the reaction was over, the mixture was diluted with water (10 mL). The formed sediment was filtered off, and recrystallized from ethanol. As a result, 0.162 g (43%) of compound **14o** was obtained (mp = 123–125 °C). ^1H NMR (DMSO-d_6, 400 MHz): δ_H 1.02 (s, 6H), 2.47 (s, 2H), 2.83 (s, 2H), 3.28 (br. s, 4H), 4.03 (br. s, 4H), 6.94–7.13 (m, 4H), 8.27 (s, 1H).MS: *m/z* ($APCI^+$) 379 ($M + H^+$). Purity (HPLC): 99,62%. Anal. Calcd ($C_{22}H_{23}FN_4O$): C, 69.82; H, 6.13; N, 14.8. Found: C, 69.74; H, 6.10; N, 14.51.

2-[4-(4-Methoxy-phenyl)-piperazin-1-yl]-7,7-dimethyl-5-oxo-5,6,7,8-tetrahydroquinoline-3-carbonitrile (14p). Compound **12b** (0.236 g, 1 mmol), 4-methoxy-phenyl-piperazine (0.23 g, 1.2 mmol), and triethylamine (0.165 mL, 1.2 mmol) were dissolved in acetonitrile (5 mL). The mixture was refluxed for 6 h, and the reaction was monitored by TLC (ethyl acetate/hexane, 1:4). When the reaction was over, the mixture was diluted with water (10 mL). The formed sediment was filtered off and recrystallized from ethanol. As a result, 0.300 g (76%) of compound **14p** was obtained (mp = 158–160 °C). ^1H NMR (DMSO-d_6, 400 MHz): δ_H 1.02 (s, 6H), 2.47 (s, 2H), 2.84 (s, 2H), 3.28 (br. s, 4H), 3.70 (s, 3H), 4.03 (br. s, 4H), 6.85 (d, J = 7 Hz, 2H), 6.95 (d, J = 7 Hz, 2H), 8.27 (s, 1H).MS: *m/z* ($APCI^+$) 391 ($M+H^+$). Purity (HPLC): 98.30%.

7,7-Dimethyl-5-oxo-2-(4-phenyl-3,6-dihydro-2H-pyridin-1-yl)-5,6,7,8-tetrahydroquinoline-3-carbonitrile (14q). Compound **12b** (0.236 g, 1 mmol), 4-phenyl-1,2,3,6-tetrahydropyridine hydrochloride (0.235 g, 1.2 mmol), and triethylamine (0.165 mL, 1.2 mmol) were dissolved in acetonitrile (5 mL). The mixture was refluxed for 6 h, and the reaction was monitored by TLC (ethyl acetate -

hexane, 1:4). When the reaction was over, the mixture was diluted with 10 mL of water. The formed sediment was filtered off and recrystallized from ethanol. As a result, 0.106 g (30%) of compound **14q** was obtained (mp = 131–133 °C). ^{1}H NMR (DMSO-d_6, 400 MHz): δ_H 1.02 (s, 6H), 2.47 (s, 2H), 2.63–2.77 (m, 2H), 2.85 (s, 2H), 4.12 (t, J = 7 Hz, 2H), 4.51 (br. s, 2H), 6.38 (br. s, 1H), 7.22–7.42 (m, 3H), 7.44–7.54 (m, 2H), 8.27 (s, 1H).MS: m/z (APCI$^+$) 358 (M + H$^+$). Purity (HPLC): 96.17%.

2-[4-(4-Fluoro-phenyl)-3,6-dihydro-2H-pyridin-1-yl]-7,7-dimethyl-5-oxo-5,6,7,8-tetrahydroquinoline-3-carbonitrile (14r). Compound **12b** (0.236 g, 1 mmol), 4-(4-fluorophenyl)-1,2,3,6-tetrahydropyridine (0.212 g, 1.2 mmol), and triethylamine (0.165 mL, 1.2 mmol) were dissolved in 5 mL of ethanol. The mixture was refluxed for 6 h, and the reaction was monitored by TLC (ethyl acetate/hexane, 1:4). When the reaction was over, the mixture was diluted with 20 mL of water and extracted with dichloromethane (3 × 10 mL). The resulting solution was filtered through a small layer of silica gel and concentrated. The residue was crystallized from ethanol. As a result, 0.155 g (41%) of compound **14r** was obtained (mp 108–110 °C). ^{1}H NMR (DMSO-d_6, 400 MHz): δ_H 1.02 (s, 6H), 2.45 (s, 2H), 2.63–2.75 (m, 2H), 2.84 (s, 2H), 4.12 (t, J = 7 Hz, 2H), 4.51 (br. s, 2H), 6.25 (br. s, 1H), 7.17 (t, J = 6 Hz, 2H), 7.52 (t, J = 6 Hz, 2H), 8.26 (s, 1H).MS: m/z (APCI$^+$) 376 (M + H$^+$). Purity (HPLC): 95.46%. Anal. Calcd ($C_{23}H_{22}FN_3O$): C, 73.58; H, 5.91; N, 11.19. Found: C, 73.06; H, 5.83; N, 11.11.

2-Benzyloxy-7,8-dihydro-6H-quinolin-5-one (17a). The compound was prepared according to ref 49. Colorless solid. mp: 80–81 °C. MS: m/z (APCI$^+$) 254 (M + H$^+$).^{1}H NMR ($CDCl_3$, TMS): δ 2.16 (m, 2H), 2.63 (t, 6.4 Hz, 2H), 3.03 (t, 6.4 Hz, 2H), 5.44 (s, 2H), 6.70 (d, 8.9 Hz, 1H), 7.3 – 7.5 (m, 5H), 8.17 (d, 8.9 Hz, 1H).

2-Benzyloxy-7,7-dimethyl-7,8-dihydro-6H-quinolin-5-one hydrochloride (17b). To a solution of benzyl alcohol (0.162 g, 1.5 mmol) in diethyl ether (10 mL) was added sodium (0.035 g, 1.5 mmol), and it was stirred at room temperature for 2.5 h. Then 2-chloro-7,7-dimethyl-7,8-dihydro-6H-quinolin-5-one (0.21 g, 1.0 mmol) was added, and the resulting mixture was stirred at 30 °C for 24 h. Water (12 mL) was added and the mixture was extracted with ethyl acetate (2 × 10 mL). The organic phase was washed with water (10 mL) and dried over magnesium sulfate; then it was filtered and evaporated under reduced pressure. The residue was purified by flash chromatography on silica gel (petroleum ether/ethyl acetate, 10:1), followed by treatment with 0.5 M dry HCl solution in diethyl ether to give the title compound in a 33% yield. MS: m/z (APCI$^+$) 282 (M + H$^+$). mpL 87–88 °C. ^{1}H NMR($CDCl_3$, TMS): δ 1.15 (s, 6H), 2.55 (s, 2H), 3.50 (s, 2H), 5.70 (s, 2H), 7.07 (d, 8.8 Hz, 1H), 7.30–7.60 (m, 5H), 8.58 (d, 8.8 Hz, 1H).

2-Benzylamino-7,7-dimethyl-7,8-dihydro-6H-quinolin-5-one (19a). 2-Chloro-7,7-dimethyl-7,8-dihydro-6H-quinolin-5-one (0.315 g, 1.5 mmol) and potassium carbonate (0.83 g, 6 mmol) were added to a solution of benzylamine (0.2 g, 1.8 mmol) in dry acetonitrile (4 mL). The mixture was stirred while boiling under reflux for 48 h. Then DMSO (3 mL) and sodium hydride (0.05 g) were added, and heating was continued for an additional 5 h. Water (10 mL) was added, and the mixture was extracted with chloroform (2 × 10 mL). The extract was dried over Na_2SO_4, filtered, and evaporated under reduced pressure. The residue was purified by flash chromatography on silica gel (chloroform/methyl alcohol, 40:1); then it was treated with dry HCl in diethyl ether to give the title compound (0.1 g, 21%) as a colorless solid with mp = 215–216 °C. MS: m/z (APCI$^+$) 281 (M + H$^+$). ^{1}H NMR ($CDCl_3$, TMS): δ 1.14 (s, 6H), 2.48 (s, 2H), 3.08 (s, 2H), 4.60 (d, 6.8 Hz, 2H), 6.64 (d, 9.4 Hz, 1H), 7.3–7.4 (m, 5H), 8.23 (d, 9.4 Hz, 1H), 9.67 (br s, 1H).

2-(4-Phenyl-piperazin-1-yl)-7,8-dihydro-6H-quinolin-5-one (19b). A mixture of compound **16a** (0.31 g, 1.7 mmol) and *N*-phenylpiperazine (5.5 g, 34 mmol) was stirred at 100 °C for 1 h (TLC control). The reaction mixture was worked out by column chromatography on silica gel (hexane/ethyl acetate, 3:1) to give 0.220 g (41%) of compound **19b** as colorless crystals (mp = 157.1–158.0 °C). ^{1}H NMR (DMSO-d_6, 400 MHz): δ_H 2.01 (t, J = 7 Hz, 2H), 2.86 (t, J = 7 Hz, 2H), 3.83 (s, 4H), 6.75–6.85 (m, 2H), 6.97 (d, J = 8 Hz, 2H), 7.23 (t, J = 8 Hz, 2H), 7.90 (d, J = 8 Hz, 1H). MS: m/z (APCI$^+$) 308 (M + H$^+$). Purity (HPLC): 99.68%.

2-Phenylethynyl-7,8-dihydro-6H-quinolin-5-one (21a). Compound **16a** (0.2 g, 1.1 mmol) was dissolved in triethylamine (5 g, 49.5 mmol), and then ethynylbenzene (0.17 g, 1.6 mmol), Pd[PPh$_3$]$_4$ (0.02 g, 0.062 mmol), and CuI (21 mg, 0.11 mmol) were added under an argon atmosphere. The mixture was stirred for 3 h at 100 °C under an argon atmosphere. Compound **21a** was isolated by column chromatography on silica gel (hexane/ethyl acetate, 50:1) and was obtained as colorless crystals (0.04 g, 15%) with mp = 121.1–121.7 °C. ^{1}H NMR (DMSO-d_6, 400 MHz): δ_H 2.13 (t, J = 7 Hz, 2H), 2.60–2.76 (m, 2H), 3.10 (t, J = 7 Hz, 2H), 7.43–7.55 (m, 3H), 7.59–7.68 (m, 3H), 8.19 (d, J = 8 Hz, 1H). MS: m/z (APCI$^+$) 248 (M + H$^+$). Purity (HPLC): 99.79%. Anal. Calcd ($C_{17}H_{13}NO$): C, 82.57; H, 5.30; N, 5.66. Found: C, 82.34; H, 5.24; N, 5.53.

2-Pyridin-2-ylethynyl-7,8-dihydro-6H-quinolin-5-one (21b). Compound **16a** (0.3 g, 1.7 mmol) was dissolved in triethylamine (10 mL). Then, 2-ethynylpyridine (0.26 g, 2.5 mmol), Pd[PPh$_3$]$_4$ (0.095 g, 0.082 mmol), and CuI (32 mg, 0.17 mmol) were added under an argon atmosphere, and the mixture was stirred for 5 h at 100 °C under an argon atmosphere. The residue was purified by column chromatography on silica gel (hexane/ethyl acetate, 1:2). As a result, 0.1 g (22%) of crystalline white compound **21b** was obtained with mp = 150–151 °C. ^{1}H NMR (DMSO-d_6, 400 MHz): δ_H 2.13 (t, J = 7 Hz, 2H), 2.60–2.76 (m, 2H), 3.10 (t, J = 7 Hz, 2H), 7.48–7.55 (m, 1H), 7.67 (d, J = 8 Hz, 1H), 8.08 (d, J = 8 Hz, 1H), 8.22 (d, J = 8 Hz, 1H), 8.66 (d, J = 4 Hz, 1H), 8.84 (s, 1H). MS: m/z (APCI$^+$) 249 (M + H$^+$). Purity (HPLC): 99.58%.

7,7-Dimethyl-2-pyridin-2-ylethynyl-7,8-dihydro-6H-quinolin-5-one (21c). Compound **16b** (0.3 g, 1.4 mmol) was dissolved in triethylamine (10 mL). Then, 3- ethynylpyridine (0.22 g, 2.1 mmol), Pd[PPh$_3$]$_4$ (0.023 g, 0.071 mmol), and CuI (26 mg, 0.14 mmol) were added under an argon atmosphere. The mixture was stirred for 3 h at 100 °C under an argon atmosphere. Then, the solvent was evaporated, and the residue was purified by column chromatography on silica gel (hexane/ethyl acetate, 1:1). As a result, 0.05 g (13%) of crystalline **21c** was obtained with mp = 108–109 °C. ^{1}H NMR (DMSO-d_6, 400 MHz): δ_H 1.08 (s, 6H), 2.62 (s, 2H), 3.06 (s, 2H), 7.54 (m, 1H), 7.71 (d, J = 10 Hz, 1H), 8.10 (d, J = 10 Hz, 1H), 8.24 (d, J = 10 Hz, 1H), 8.68 (d, J = 6 Hz, 1H), 8.87 (s, 1H). MS: m/z (APCI$^+$) 277 (M + H$^+$). Purity (HPLC): 99.20%.

6,6-Dimethyl-2-phenylethynyl-7,8-dihydro-6H-quinolin-5-one (21d). Sodium hydride (0.048 g, 1.2 mmol, 1.5 equiv) was added in an argon atmosphere to a solution of 2-phenylethynyl-7,8-dihydro-6H-quinolin-5-one (**21a**) (0.2 g, 0.8 mmol, 1 equiv) in dry THF (5 mL), and the mixture was stirred for 30 min at room temperature. Then iodomethane (0.16 g, 1.2 mmol, 1.5 equiv) was added to the reaction mixture, and stirring was continued for 3 h at room temperature. Then the reaction mixture was evaporated, and the residue was subjected to column chromatography on silica gel (60–100 μ, l = 20 cm, d = 2 cm, hexane/ethyl acetate 3:1). As a result, 0.033 g (13%) of **21d** was obtained. ^{1}H NMR (400 MHz, $CDCl_3$): δ 1.25 (6H, s), 2.06 (2H, t), 3.20 (2H, t), 7.33–7.43 (3H, m), 7.49 (1H, d), 7.63 (2H, d), 8.29 (1H, d). MS: m/z (CI MS) 276 (M + H$^+$). Purity (HPLC): 95.83%.

7,7-Dimethyl-3-nitro-2-(4-phenyl-3,6-dihydro-2H-pyridin-1-yl)-7,8-dihydro-6H-quinolin-5-one (24b). To the solution of the compound **23** (0.12 g, 0.47 mmol) in acetonitrile (10 mL), diisopropylethylamine (0.15 g, 1.1 mmol) and 4-phenyl-1,2,3,6-tetrahydro-pyridine hydrochloride (0.138 g, 0.7 mmol) were added. The mixture was refluxed for 3 h. The solvent was evaporated. The residue was purified by column chromatography on silica gel (hexane/ethyl acetate, 4:1). As a result, compound **24** was obtained (0.06 g, 34%) as an oil. ^{1}H NMR ($CDCl_3$, TMS, 400 MHz): δ_H 1.25 (s, 3H), 1.28 (s, 3H), 2.70 (s, 2H), 2.90 (d, J = 20 Hz, 1H), 3.10 (d, J = 20 Hz, 1H), 4.08 (s, 2H), 4.35 (s, 2H), 5.19 (s, 1H), 6.19 (br. s, 1H), 6.62 (d, J = 11 Hz, 1H), 7.20–7.55 (m, 5H), 8.09 (d, J = 11 Hz, 1H). MS: m/z (APCI$^+$) 378 (M + H$^+$).

3-Bromo-2-cyclopentylamino-7,7-dimethyl-7,8-dihydro-6H-quinolin-5-one (27a). Compound **26** (0.15 g, 0.45 mmol) and cyclopentylamine (0.38 g, 4.5 mmol) were fused at 80 °C for 2 h. Purification of the cake by column chromatography on silica gel (hexane/ethyl acetate, 2:1) gave 0.053 g (34%) of light yellow crystalline compound **27a** (mp = 176–177 °C). ^{1}H NMR (DMSO-d_6, 400 MHz): δ_H 1.20 (s, 3H), 1.27 (s, 3H), 1.47–1.85 (m, 6H), 2.03–2.15 (m, 2H), 2.61 (d, J = 18 Hz, 1H), 3.12 (d, J = 18 Hz, 1H), 4.04–4.16 (m, 1H), 4.29 (s, 1H), 5.10–5.23 (m, 1H), 6.36 (d, J = 10 Hz, 1H), 8.07 (d, J = 10 Hz, 1H). MS: m/z (APCI$^+$) 337 (M + H$^+$). Purity (HPLC): 96.19%.

3-Bromo-2-[4-(4-fluoro-phenyl)-piperazin-1-yl]-7,7-dimethyl-7,8-dihydro-6H-quinolin-5-one (27b). Compound **26** (0.1 g, 0.3 mmol) and 1-(4-fluoro-phenyl)-piperazine (0.5 g, 3 mmol) were fused at 80 °C for 1 h. Purification of the residue by column chromatography on silica gel (hexane/ethyl acetate, 3:2 v/v) gave 0.02 g (16%) of compound **27b** as a colorless oil. ^{1}H NMR (DMSO-d_6, 400 MHz): δ_H 1.11 (s, 6H), 2.45 (s, 2H), 2.82 (s, 2H), 3.36 (br. s, 4H), 3.74 (br. s, 4H), 6.86–7.05 (m, 4H), 8.29 (s, 1H). MS: m/z (APCI$^+$) 432 (M + H$^+$).

3-Chloro-2-cyclopentylamino-7,7-dimethyl-7,8-dihydro-6H-quinolin-5-one (27c). (a) Synthesis of 3-Chloro-7,7-dimethyl-7,8-dihydro-1H,6H-quinoline-2,5-dione. *N*-chlorosuccinimide (0.8 g, 5.5 mmol) was added to a solution of 7,7-dimethyl-7,8-dihydro-1*H*,6*H*-quinoline-2,5-dione (1.0 g, 5.0 mmol) in 1,2-dichloroethane (50 mL). The reaction mixture was refluxed for 8 h. Then the solvent was removed on a rotary evaporator. The residue was crystallized with ethanol (5 mL). The colorless crystals formed were filtered off and dried on air to give 0.3 g (25%) of the title compound. MS: m/z (APCI$^+$) 226 (M + H$^+$).

(b) Synthesis of 2-Bromo-3-chloro-7,7-dimethyl-7,8-dihydro-6H-quinolin-5-one. $POBr_3$ (0.46 g, 1.6 mmol) was added to a solution of 3-chloro-7,7-dimethyl-7,8-dihydro-1*H*,6*H*-quinoline-2,5-dione (0.3 g, 1.3 mmol) in acetonitrile (25 mL). The reaction mixture was refluxed for 5 h. Then the solvent was evaporated. The residue was dissolved in dichloromethane (20 mL) and washed with 10% aqueous potassium carbonate and water. The organic layer was separated, dried over sodium sulfate, and concentrated. The residue was purified by column chromatography on silica gel (hexane/ethyl acetate, 1:1) to give 0.06 g (16%) of the title compound as a light yellow oil. MS: m/z (APCI$^+$) 289 (M+H$^+$).

(c) Synthesis of 3-Chloro-2-cyclopentylamino-7,7-dimethyl-7,8-dihydro-6H-quinolin-5-one (27c). A mixture of 2-bromo-3-chloro-7,7-dimethyl-7,8-dihydro-6H-quinolin-5-one (0.06 g, 0.21 mmol) and cyclopentylamine (0.18 g, 2.1 mmol) was fused at 80 °C for 2 h. Purification of the cake by column chromatography on silica gel (hexane/ethyl acetate, 2:1) resulted in 0.032 g (45%) of light yellow crystalline **27c** (mp = 80–81 °C). ^{1}H NMR ($CDCl_3$, TMS, 400 MHz): δ_H 1.08 (s, 6H), 2.40 (s, 2H), 2.78 (s, 2H), 4.48 (m, 1H), 5.42 (br. s, 1H), 7.98 (s, 1H). MS: m/z (APCI$^+$) 293 (M + H$^+$). Purity (HPLC): 95.91%.

2-Cyclopentylamino-7,7-dimethyl-5-oxo-5,6,7,8-tetrahydro-quinoline-3-carboxylic acid (28). A solution of compound **14d** (0.283 g, 1.0 mmol) in a mixture of HCl/AcOH/H_2SO_4/H_2O (1/1/1/1 v/v; 20 mL) was refluxed for 12 h (TLC control; ethyl acetate/hexane, 1:2). Then, mixture was cooled and carefully basified with aqueous NH_3 to pH 7–8. The formed precipitate was filtered off, washed with water, and dried in air to give 0.21 g (70%) of compound **28** as white solid (mp = 196–197 °C). ^{1}H NMR (DMSO-d_6, 400 MHz): δ_H 1.00 (s, 6H), 1.35–1.76 (m, 6H), 1.92–2.06 (m, 2H), 2.32 (s, 2H), 2.73 (s, 2H), 4.35–4.51 (m, 1H), 8.39 (s, 1H), 9.64 (br. s, 1H). MS: m/z (APCI$^+$) 303 (M + H$^+$). Purity (HPLC): 99.61%.

2-Cyclopentylamino-7,7-dimethyl-5-oxo-5,6,7,8-tetrahydro-quinoline-3-carboxylic acid dimethylamide (29). TBTU (0.13 g, 0.4 mmol), dimethylamine hydrochloride (0.03 g, 0.35 mmol), and triethylamine (0.2 mL) were added to a solution of compound **28** (0.1 g, 0.3 mmol) in acetonitrile (4 mL). The mixture was stirred at room temperature for 2 h (TLC control; ethyl acetate/hexane, 1:2). Then, the mixture was diluted with water (15 mL) and extracted with dichloromethane (3 × 10 mL). The extract was dried over Na_2SO_4 and evaporated. The residue was purified by column chromatography on silica gel (ethyl acetate/hexane, 1:5) to give 0.052 g (50%) of compound **29** as a white solid (mp = 133–134 °C). ^{1}H NMR (DMSO-d_6, 400 MHz): δ_H 1.02 (s, 6H), 1.41–1.76 (m, 6H), 1.89–2.06 (m, 2H), 2.38 (s, 2H), 2.77 (s, 2H), 2.94 (s, 6H), 4.37–4.51 (m, 1H), 6.87 (d, J = 11 Hz, 1H), 7.71 (s, 1H). MS: m/z (APCI$^+$) 330 (M + H$^+$). Purity (HPLC): 99.60%.

2-[4-(4-Fluoro-phenyl)-3,6-dihydro-2H-pyridin-1-yl]-7,7-dimethyl-3-morpholin-4-yl-7,8-dihydro-6H-quinolin-5-one (31). A mixture of compound **30** (0.15 g, 0.35 mmol), sodium *tert*-pentoxide (0.093 g, 0.85 mmol), morpholine (0.061 g, 0.7 mmol), bis(dibenzylideneacetone)palladium (0.03 g, 0.052 mmol), and 2-(di-*t*-butylphosphino)biphenyl (0.016 g, 0.053 mmol) in tetrahydrofuran (5 mL) was stirred under an argon atmosphere at 66 °C for 8 h. Then, the reaction mixture was concentrated under reduced pressure. The residue was purified by column chromatography on silica gel (hexane/ethyl acetate, 5:1). As a result, 0.026 g (17%) of compound **31** was isolated as light yellow oil. ^{1}H NMR (DMSO-d_6, 400 MHz): δ_H 1.10 (s, 6H), 2.42 (s, 2H), 2.65 (s, 2H), 2.81 (s, 2H), 3.03 (s, 4H), 3.86 (s, 4H), 4.02 (t, J = 7 Hz, 1H), 4.40 (s, 1H), 6.15 (s, 1H), 7.03 (t, J = 12 Hz, 2H), 7.38 (t, J = 12 Hz, 2H), 7.67 (s, 1H). MS: m/z (APCI$^+$) 436 (M + H$^+$).

2-Cyclopentylamino-7,7-dimethyl-3-pyrimidin-5-yl-7,8-dihydro-6H-quinolin-5-one (33a). To a solution of compound **32** (0.22 g, 0.8 mmol), pyridine (0.135 g, 1.7 mmol), and diisopropylethylamine (1.18 g, 1.4 mmol) in dichloromethane (10 mL) trifluoromethanesulfonic anhydride (0.38 g, 1.4 mmol) was added. The reaction mixture was stirred at room temperature for 3 h; then, the solvent was evaporated. Purification of the residue by column chromatography on silica gel (hexane/ethyl acetate, 3:1) gave 0.25 g (80%) of the product as a dark oil. A mixture of this oil (0.25 g, 0.64 mmol), cyclopentylamine (0.38 g, 4.5 mmol) and diisopropylethylamine (0.12 g, 0.9 mmol) in acetonitrile (10 mL) was refluxed for 4 h. Then the solvent was removed in vacuo, and the residue was purified by HPLC to give colorless crystalline compound **33** (0.32 g, 17%, mp = 191–193 °C). ^{1}H NMR (DMSO-d_6, 400 MHz): δ_H 1.12 (s, 6H), 1.27–1.41 (m, 2H), 1.57–1.73 (m, 4H), 2.03–2.15 (m, 2H), 2.42 (s, 2H), 2.87 (s, 2H), 4.45–4.55 (m, 1H), 4.71 (br. s, 1H), 7.26 (s, 1H), 7.83 (s, 1H), 8.78 (s, 2H), 9.23 (s, 1H). MS: m/z (APCI$^+$) 337 (M + H$^+$). Purity (HPLC): 100%.

2-Cyclopentylamino-7,7-dimethyl-3-(2H-tetrazol-5-yl)-7,8-dihydro-6H-quinolin-5-one (33b). To a solution of **14d** (0.566 g, 2 mmol) in dry DMF (5 mL), sodium azide (0.260 g, 4 mmol) and ammonium chloride (0.214 g, 4 mmol) were added. The mixture was refluxed for 3 h (TLC control, ethyl acetate/hexane, 1:2). Then, the mixture was diluted with water (20 mL) and acidified with acetic acid to pH 5. The formed precipitate was filtered off and crystallized with ethanol to give 0.45 g (69%) of **34** (mp 269–271 °C). MS: m/z (APCI$^+$) 327 (M + H$^+$). Purity (HPLC): 99.47%.

2-Phenylethynyl-5,6,7,8-tetrahydro-quinolin-5-ol (34). To a suspension of the compound **27a** (0.12 g, 0.48 mmol) in isopropyl alcohol (25 mL), $NaBH_4$ (0.2 g, 5.3 mmol) was added, and the mixture was stirred for 5 h at RT (room temperature). Then, the solvent was evaporated under reduced pressure. The residue was dissolved in chloroform (50 mL), washed with water, and dried over Na_2SO_4. The chloroform was evaporated. As a result of HPLC separation, 0.12 g (99%) of compound **34** was obtained as an oil. ^{1}H NMR (DMSO-d_6, 400 MHz): δ_H 1.65–1.87 (m, 2H), 1.95–2.07 (m, 2H), 2.80–2.95 (m, 2H), 4.69 (br. s, 1H), 7.45–7.53 (m, 3H), 7.56 (d, J = 8 Hz, 1H), 7.60–7.68 (m, 3H), 7.93 (d, J = 8 Hz, 1H). MS: m/z (APCI$^+$) 250 (M + H$^+$). Anal. Calcd ($C_{17}H_{15}NO$) C, 81.90; H, 6.06; N, 5.62. Found: C, 81.60; H, 5.93; N, 5.41.

(*S*)-2-Phenylethynyl-5,6,7,8-tetrahydro-quinolin-5-ol (34a) and (*R*)-2-Phenylethynyl-5,6,7,8-tetrahydro-quinolin-5-ol (34b). Racemic mixture of isomers of 2-phenylethynyl-5,6,7,8-tetrahydro-quinolin-5-ol (**34**) (0.15 g, 0.6 mmol) was separated by HPLC (column Chiralpak AD-H 4.6 × 250 mm 5 mkm; mobile phase hexane/IPA 90/10; flow1.0 mL/min; detection UV at 240 nm; ambient temperature) to give 0.064 g (43%) of (*S*)-2-phenylethynyl-5,6,7,8-tetrahydro-quinolin-5-ol (**34a**) (e.e. > 99.5%) and 0.069 g (46%) of (*R*)-2-phenylethynyl-5,6,7,8-tetrahydro-quinolin-5-ol (**34b**)

(e.e. > 99.5%) as oils. ^{1}H NMR (400 MHz, $CDCl_3$): δ 1.78–1.98 (3H, m), 2.00–2.17 (2H, m), 2.86–3.08 (2H, m), 4.77–4.87 (1H, m), 7.30–7.42 (4H, m), 7.55–7.63 (2H, m), 7.77 (1H, d). CI MS: *m*/*z* 250 ($M + H^+$).

2-Phenylethynyl-5,6,7,8-tetrahydro-quinoline (35). A solution of the compound **34** (0.12 g, 0.48 mmol), DMAP (0.06 g, 0.049 mmol), Et_3N (0.1 mL, 0.1 mmol), and tosyl chloride (0.2 g, 0.1 mmol) in dichloroethane (20 mL) was heated at 70 °C for 3 days. Then, the solvent was evaporated. The residue was purified by column chromatography on silica gel (60–100 μm, hexane/ethyl acetate, 2:1). As a result, the Tos-derivative of **34** (0.1 g, 51%) was obtained as an oil. To a solution of the obtained compound (0.1 g, 0.25 mmol) in DMSO (1 mL), $NaBH_4$ (0.05 g, 1.2 mmol) was added. The reaction mixture was stirred at 60 °C for 6 h, dissolved in chloroform (30 mL), and washed with water (3 × 25 mL). The organic layer was dried over Na_2SO_4, and the solvent was evaporated. The product was isolated by column chromatography on silica gel (60–100 μm, hexane/ethyl acetate, 2:1). As a result, compound **34** (0.03 g, 52%) was obtained as a colorless oil. ^{1}H NMR (DMSO-d_6, 400 MHz): δ_H 1.65–2.07 (m, 4H), 2.75–2.85 (m, 2H), 2.92–3.02 (m, 2H), 7.23–7.39 (m, 5H), 7.55–7.63 (m, 2H). MS: *m*/*z* (APCI$^+$) 234 ($M + H^+$).

6-Phenylethynyl-nicotinic acid methyl ester (36). Ethynylbenzene (0.265 g (2.6 mmol), $Pd(Ph_3P)_2Cl_2$ (0.07 g, 0.1 mmol), and CuI (0.04 g, 0.2 mmol) were added to 6-chloro-nicotinic acid methyl ester (0.342 g, 2 mmol) in 5 mL of triethylamine under argon atmosphere. Then, the mixture was refluxed for 8 h under an argon atmosphere and was monitored by TLC (ethyl acetate/hexane, 1:3). Thereafter, the mixture was cooled, and the sediment that formed was filtered off. The crude material was dissolved in dichloromethane and was purified by column chromatography on silica gel (dichloromethane). As a result, 0.165 g (35%) of compound **36** was obtained as a white solid (mp = 138–140 °C). ^{1}H NMR (DMSO-d_6, 400 MHz): δ_H 3.92 (s, 3H), 7.44–7.54 (m, 3H), 7.65 (d, J = 7 Hz, 2H), 7.78 (d, J = 7 Hz, 1H), 8.32 (d, J = 7 Hz, 1H), 9.09 (s, 1H). MS: *m*/*z* (APCI$^+$) 238 ($M + H^+$). Purity (HPLC): 100%.

5-Methoxy-2-phenylethynyl-5,6,7,8-tetrahydro-quinoline (37). Sodium hydride (0.048 g, 1.2 mmol, 1.5 equiv) was added in an argon atmosphere to a solution of 2-phenylethynyl-5,6,7,8-tetrahydro-quinolin-5-ol (**21a**) (0.2 g, 0.8 mmol, 1 equiv) in dry dioxane (5 mL), and the mixture was stirred for 30 min at room temperature. Then iodomethane (0.16 g, 1.2 mmol, 1.5 equiv) was added to the reaction mixture, and stirring was continued for 3 h at room temperature. Then the reaction mixture was evaporated, and the residue was subjected to column chromatography on silica gel (60–100 μ, l = 20 cm, d = 2 cm, hexane/ethyl acetate 2:1). As a result, 0.065 g (31%) of crystalline **37** was obtained with mp = 94 °C. ^{1}H NMR (400 MHz, $CDCl_3$): δ 1.75–2.17 (4H, m), 2.86–3.09 (2H, m), 3.47 (3H, s), 4.30–4.40 (1H, m), 7.30–7.42 (4H, m), 7.56–7.65 (2H, m), 7.70 (1H, d). MS: *m*/*z* (CI MS) 264 ($M + H^+$). Purity: (HPLC): 100%.

(B) Pharmacology Assays. (Cell culture, cell preparation, membrane preparation, and compound preparation are reported in the Supporting Information.)

mGluR5 Assay: Calcium FLIPR Studies. The increase of intracellular calcium after stimulation with the mGluR5 agonist DHPG or L-quisqualate was measured using a fluorometric imaging plate reader (FLIPR tetra) and the Ca-Kit (both Molecular Devices, CA). Prior to the addition of agonist or antagonist, the medium was aspirated, and the cells were loaded for 2 h at RT with 150 μL of loading buffer consisting of Ca-sensitive dye (MD R8033) reconstituted in sodium chloride (123 mM), potassium chloride (5.4 mM), magnesium chloride (0.8 mM), calcium chloride (1.8 mM), D-glucose (15 mM), and HEPES (20 mM), pH 7.3. Subsequently, the plates were transferred to FLIPR to detect calcium increase with the addition of DHPG (300 μM) or L-quisqualate (100 nM) measured as relative fluorescence units (RFU). Compounds were preincubated for 10 min prior to the addition of the agonist. Effects on the human mGluR5 were tested with L-glutamate as agonist and a preincubation time of 5 min. The human mGluR5 was expressed in a stable CHO cell line under control of an inducible promoter (LacSwitchII, Stratagene). In this case, the Ca-Kit contained glutamic-pyruvate transferase (GPT), Na-pyruvate, and pyridoxal phosphate to avoid accumulation of glutamate during Ca-dye loading. Positive allosteric modulators were characterized in two ways. First, the EC_{50} of the potentiation was tested by preincubation of concentration range of the modulator and subsequent stimulation with a fixed, low concentration of agonist ($\sim EC_{20}$). Second, the increase in agonist potency by a positive modulator was determined by running two agonist curves in parallel: one without and one with a preincubated modulator. This potency increase was expressed as a left shift and determined as the ratio of the EC_{50} values.

mGluR1 Assay: Accumulation of [^{3}H]-Inositol Phosphates. After cerebellar granule cells were cultured for 7 days, BEM was removed, and inositol-free DMEM (ICN) supplemented with [^{3}H]myo-inositol (0.5 μCi/well; Perkin-Elmer) was added. After 48 h, the medium was replaced with 100 μL of Locke's buffer (plus 20 mM Li^+, pH 7.4) and incubated for 15 min at 37 °C before replacement with agonists/antagonists in Locke's buffer. The incubation (45 min at 37 °C) was terminated by replacement of the Locke's solutions with 100 μL of 0.1 M HCl (10 min on ice). The 96-well plates can be frozen at −20 °C at this stage until further analysis. Home-made resin exchange columns (AG1-X8 Biorad, 140–14 444) were used to separate labeled inositol phosphates by elution with 1 mL of 1 M ammonium formate/0.1 M formic acid into 24-well visiplates (Perkin-Elmer). Scintillation liquid (UltimaFlow AF, Perkin-Elmer) was added, and the plate was sealed and vortexed before the radioactivity was determined by conventional liquid scintillation counting (Microbeta,Perkin-Elmer) as disintegrations per minute (DPM). At least three independent experiments were performed.

mGluR5 Binding Assay: [^{3}H]MPEP] Assay. On the day of assay, the membranes were thawed and washed four times by resuspension in 50 mM Tris-HCl, pH 8.0, and centrifugation at 48 000 × g for 20 min, and finally, they were resuspended in 50 mM Tris-HCl, pH 7.5. The amount of protein in the final membrane preparation (250–500 μg/ml) was determined according to the method of Lowry.[50] Incubations were started by the addition of [^{3}H]-MPEP (50.2 Ci/mmol, 5 nM, Tocris) to vials with 125–250 μg of protein (total volume 0.5 mL) and various concentrations of the agents. The incubations were continued at room temperature for 60 min (equilibrium was achieved under the conditions used). Nonspecific binding was defined by the addition of unlabeled MPEP (10 μM). Incubations were terminated using a Millipore filter system. The samples were rinsed twice with 4 mL of ice cold assay buffer over glass fiber filters (Schleicher and Schuell) under a constant vacuum. Following the separation and rinse, the filters were placed into scintillation liquid (5 mL of Ultima Gold), and the radioactivity retained on the filters was determined with a conventional liquid scintillation counter (Hewlett-Packard, Liquid Scintillation Analyzer). The solubility of most of the compounds was increased by using up to 5% DMSO in the final assay solution.

Specific binding was extremely high, that is, normally >85% and essentially independent of buffer (Tris or HEPES oth 50 mM) and pH (6.8–8.9). There was a clear saturable protein dependence, and the chosen protein concentration used for subsequent assays (250–500 μg/mL) was within the linear portion of this dependence. Cold MPEP displaced hot ligand with an IC_{50} of 18.8 ± 4.1 nM. The K_d of [^{3}H]MPEP of 13.6 nM was determined by Scatchard analysis and used according to the Cheng Prussoff relationship to calculate the affinity of displacers as K_d values (IC_{50} of cold MPEP equates to a K_i of 13.7 nM). B_{max} was 0.56 pm/mg protein. Since this assay is very stable, only two independent experiments were performed.

(C) Computational Chemistry: Generation of a Pharmacophore Model for mGluR1. (The generation of the mGluR1 homology model and the alignment of TM helices and EL2 of rat mGluR1 to the bovine rhodopsin structural template is given in the Supporting Information.)

Flexible Alignment of 1, 2, and 3 by Application of MOE (Chemical Computing Group). After generation of 3D structures for all molecules (**1**, **2**, and **3**), using a favored force field for small compounds (MMFF94), molecules **1** and **2** were superimposed in a flexible manner using the *Flexible Alignment* tool included in the MOE software package (version 2003.02, Chemical Computing Group) according to the following settings: iteration limit, 200 attempts; failure limit, 20 configurations in a row; energy cutoff, 10.0 kcal/mol greater than the minimum generated value; configuration limit, 1000 alignment configurations; α, 2.5; gradient test, 0.01; rmsd tolerance, 0.5Å; maximum steps, 500 energy minimization steps; similarity terms, H-bond donor/acceptor (1/1), aromaticity (3), acid/base (1), hydrophobe (1), polar hydrogens (1), and volume (3)). Several orientations have been calculated including their corresponding energy values. One orientation with a low energy value and a reasonable overlay (i.e., the most complete overlay with respect to the core structures) was manually selected and both molecules were kept in a fixed position relative to each other for further alignments. In the next step, molecule **2** was superimposed onto this orientation, and a sensible overlay was saved and fixed for the next alignment procedure. Eventually, the remaining structure was aligned on this orientation, resulting in a final alignment for allosteric mGluR1 antagonists (Figure 2). Alignment settings remained unchanged throughout the whole process.

Assignment of the Pharmacophore Elements. A pharmacophore hypothesis was established based upon this flexible overlay using the *Pharmacophore Query Editor* of the MOE software. This tool displays certain chemical properties (H-bond donor/acceptor, etc.) of nonhydrogen atoms of each molecule to be edited, which are here referred to as annotation points. For this model, the default PCH-type was employed. Here, annotation points of the same label, which occur in all molecules at nearly the same spatial position were presumed to be important. Query features were then assigned to these important annotation points. A query feature denotes a point in space with a radiuslike tolerance on spatial proximity and an associated expression. The expression and the radius of each query feature were manually edited. The diameter of each tolerance radius was chosen to be sufficiently large to cover identical annotation points of every molecule in that region.

Virtual Screening of a Compound Database. In the search for new ligands, we virtually screened the Asinex Gold compound collection, version of April 2003 (Asinex Ltd., Moscow, Russia, http://www.asinex.com), which contained 194 563 molecules. All molecules which did not fulfill the criteria of Lipinski's Rule of Five were removed from the database.[51]

Acknowledgment. The authors would like to thank the Merz Compound Management Group for their great support and for numerous HPLC measurements to assess the purity of the compounds. Furthermore, we gratefully acknowledge the help of Sylvia Willy, Andrea Baude, Sabine Denk, and Christina Wollenburg for performing functional mGluR1/5 experiments and mGluR5 binding assays.

Supporting Information Available: Table listing the analytical techniques used to determine degree of purity for all target compounds, the synthesis procedures of all intermediate products, a detailed description of the cell culture, membrane preparation and compound preparation, and a detailed description of the generation of the mGluR1 homology model and the alignment of TM helices and EL2 of rat mGluR1 to the bovine rhodopsin structural template. This material is available free of charge via the Internet at http://pubs.acs.org.

References

(1) Klabunde, T.; Hessler, G. Drug design strategies for targeting G-protein-coupled receptors. *ChemBioChem* **2002**, *3* (10), 928–944.

(2) Wess, J. Molecular basis of receptor/G-protein-coupling selectivity. *Pharmacol. Ther.* **1998**, *80* (3), 231–264.

(3) Brown, E. M.; Gamba, G.; Riccardi, D.; Lombardi, M.; Butters, R.; Kifor, O.; Sun, A.; Hediger, J.; Lytton, M. A.; Hebert, S. C. Cloning and characterization of an extracellular Ca21-sensing receptor from bovine parathyroid. *Nature* **1993**, *366*, 575–580.

(4) Jones, K. A.; Borowsky, B.; Tamm, J. A.; Craig, D. A.; Durkin, M. M.; Dai, M.; Yao, W. J.; Johnson, M.; Grunwaldsen, C.; Huang, L. Y.; Tang, C.; Shen, Q.; Salon, J. A.; Morse, K.; Laz, T.; Smith, K. E.; Nagarathnam, D.; Noble, S. A.; Branchek, T. A.; Gerald, C. GABA(B) receptors function as a heteromeric assembly of the subunits GABA(B)R1 and GABA(B)R2. *Nature* **1998**, *396* (6712), 674–679.

(5) Kaupmann, K.; Malitschek, B.; Schuler, V.; Heid, J.; Froestl, W.; Beck, P.; Mosbacher, J.; Bischoff, S.; Kulik, A.; Shigemoto, R.; Karschin, A.; Bettler, B. GABA(B)-receptor subtypes assemble into functional heteromeric complexes. *Nature* **1998**, *396* (6712), 683–687.

(6) Charest, P. G.; Oligny-Longpré, G.; Bonin, H.; Azzi, M.; Buvier, M. The V2 vasopressin receptor stimulates ERK1/2 activity independently of heterotrimeric G protein signalling. *Cell. Signal.* **2007**, *19* (1), 32–41.

(7) Palmer, R. K. The pharmacology and signaling of bitter, sweet, and umami taste sensing. *Mol Interv.* **2007**, *7* (2), 87–98.

(8) Hoon, M. A.; Adler, E.; Lindemeier, J.; Battey, J. F.; Ryba, N. J.; Zuker, C. S. Putative mammalian taste receptors: a class of taste-specific GPCRs with distinct topographic selectivity. *Cell* **1999**, *96* (4), 541–551.

(9) Nakanishi, S.; Masu, M. Molecular diversity and functions of glutamate receptors. *Annu. Rev. Biophys. Biomol. Struct.* **1994**, *23*, 319–348.

(10) Hollmann, M.; Heinemann, S. Cloned glutamate receptors. *Annu. Rev. Neurosci.* **1994**, *17*, 31–108.

(11) Pin, J. P.; Galvez, T.; Prezeau, L. Evolution, structure, and activation mechanism of family 3/C G-protein-coupled receptors. *Pharmacol. Ther.* **2003**, *98* (3), 325–354.

(12) O'Hara, P. J.; Sheppard, P. O.; Thogersen, H.; Venezia, D.; Haldeman, B. A.; McGrane, V.; Houamed, K. M.; Thomsen, C.; Gilbert, T. L.; Mulvihill, E. R. The ligand-binding domain in metabotropic glutamate receptors is related to bacterial periplasmic binding proteins. *Neuron* **1993**, *11* (1), 41–52.

(13) Kew, J. N. Positive and negative allosteric modulation of metabotropic glutamate receptors: emerging therapeutic potential. *Pharmacol Ther.* **2004**, *104* (3), 233–244.

(14) Lavreysen, H.; Pereira, S. N.; Leysen, J. E.; Langlois, X.; Lesage, A. S. Metabotropic glutamate 1 receptor distribution and occupancy in the rat brain: a quantitative autoradiographic study using [3H]R214127. *Neuropharmacology* **2004**, *46* (5), 609–619.

(15) Pin, J.-P.; Acher, F. The metabotropic glutamate receptors: Structure, activation mechanism and pharmacology. *Curr. Drug Targets: CNS Neurol. Disord.* **2002**, *1* (3), 297–317.

(16) Conn, P. J.; Pin, J.-P. Pharmacology and functions of metabotropic glutamate receptors. *Annu. Rev. Pharmacol. Toxicol* **1997**, *37*, 205–237.

(17) Nicoletti, F.; Bruno, V.; Copani, A.; Casabona, G.; Knöpfel, T. Metabotropic glutamate receptors: a new target for the therapy of neurodegenerative disorders. *Trends Neurosci.* **1996**, *19* (7), 267–271.

(18) Young, M. R.; Fleetwood-Walker, S. M.; Mitchell, R.; Munro, F. E. Evidence for a role of metabotropic glutamate receptors in sustained nociceptive inputs to rat dorsal horn neurons. *Neuropharmacology* **1994**, *33* (1), 141–144.

(19) Varney, M. A.; Gereau, R. W. I. Metabotropic glutamate receptor involvement in models of acute and persistent pain: Prospects for the development of novel analgesics. *Curr. Drug Targets: CNS Neurol. Disord.* **2002**, *1* (3), 283–296.

(20) Spooren, W. P. J. M.; Vassout, A.; Neijt, H. C.; Kuhn, R.; Gasparini, F. Anxiolytic-like effects of the prototypical metabotropic glutamate receptor 5 antagonist 2-methyl-6-(phenylethynyl)pyridine in rodents. *J. Pharmacol. Exp. Ther.* **2000**, *295* (3), 1267–1275.

(21) Chiamulera, C.; Epping-Jordan, M. P.; Zocchi, A.; Marcon, C.; Cottiny, C. Reinforcing and locomotor stimulant effects of cocaine are absent in mGluR5 null mutant mice. *Nat. Neurosci.* **2001**, *4* (9), 873–874.

(22) Spooren, W. P. J. M.; Gasparini, F.; Bergmann, R.; Kuhn, R. Effects of the prototypical mGlu(5) receptor antagonist 2-methyl-6-(phenylethynyl)-pyridine on rotarod, locomotor activity and rotational responses in unilateral 6-OHDA-lesioned rats. *Eur. J. Pharmacol.* **2000**, *406* (3), 403–410.

(23) Chavez-Noriega, L. E.; Schaffhauser, H. J. L.; Campbell, U. C. Metabotropic glutamate receptors: potential drug targets for the treatment of schizophrenia. *Curr. Drug Targets CNS Neurol. Disord.* **2002**, *1* (3), 261–281.

(24) Moghaddam, B. Targeting metabotropic glutamate receptors for treatment of the cognitive symptoms of schizophrenia. *Psychopharmacol.* **2004**, *174* (1), 39–44.

(25) Noeske, T.; Gutcaits, A.; Parsons, C. G.; Weil, T. Allosteric Modulation of Family 3 GPCRs. *QSAR Comb. Sci.* **2006**, *25* (2), 134–146.

(26) Palczewski, K.; Kumasaka, T.; Hori, T.; Behnke, C. A.; Motoshima, H.; Fox, B. A.; Trong, I. L.; Teller, D. C.; Okada, T.; Stenkamp, R. E.; Yamamoto, M.; Miyano, M. Crystal structure of rhodopsin: A G protein-coupled receptor. *Science* **2000**, *289* (5480), 739–745.

(27) Gribbon, P.; Sewing, A. Fluorescence readouts in HTS: no gain without pain. *Drug Discov. Today* **2003**, *8* (22), 1035–1043.

(28) Pagano, A.; Ruegg, D.; Litschig, S.; Stoehr, N.; Stierlin, C.; Heinrich, M.; Floersheim, P.; Prezeau, L.; Carroll, F.; Pin, J. P.; Cambria, A.; Vranesic, I.; Flor, P. J.; Gasparini, F.; Kuhn, R. The non-competitive antagonists 2-methyl-6- (phenylethynyl)pyridine and 7-hydroxyiminocyclopropan [b]chromen-1a-carboxylic acid ethyl ester interact with overlapping binding pockets in the transmembrane region of group I metabotropic glutamate receptors. *J. Biol. Chem.* **2000**, *275*, 33750–33758.

(29) Mabire, D.; Coupa, S.; Adelinet, C.; Poncelet, A.; Simonnet, Y.; Venet, M.; Wouters, R.; Lesage, A. S.; Beijsterveldt, L. V.; Bischoff, F. Synthesis, structure-activity relationship, and receptor pharmacology of a new series of quinoline derivatives acting as selective, noncompetitive mGlu1 antagonists. *J. Med. Chem.* **2005**, *48* (6), 2134–2153.

(30) Knoflach, F.; Mutel, V.; Jolidon, S.; Kew, J. N.; Malherbe, P.; Vieira, E.; Wichmann, J.; Kemp, J. A. Positive allosteric modulators of metabotropic glutamate 1 receptor: Characterization, mechanism of action, and binding site. *Proc. Natl. Acad. Sci. U.S.A.* **2001**, *98* (26), 13402–13407.

(31) Lavreysen, H.; Janssen, C.; Bischoff, F.; Langlois, X.; Leysen, J. E.; Lesage, A. S. [3H]R214127: A novel high-affinity radioligand for the mGlu1 receptor reveals a common binding site shared by multiple allosteric antagonists. *Mol. Pharmacol.* **2003**, *63* (5), 1082–1093.

(32) Noeske, T.; Jirgensons, A.; Stachenkovs, I.; Renner, S.; Jaunzeme, I.; Trifanova, D.; Hechenberger, M.; Bauer, T.; Schneider, G.; Parsons, C. G.; Weil, T. Virtual screening for selective allosteric mglur1 antagonists and structure−activity relationship investigations for coumarine derivatives *ChemMedChem* **2007**, in press.

(33) Asinex_Gold_Collection, http://www.asinex.com, 2003.

(34) Gasparini, F.; Andres, H.; Flor, P. J.; Heinrich, M.; Inderbitzin, W.; Lingenhohl, K.; Muller, H.; Munk, V. C.; Omilusik, K.; Stierlin, C.; Stoehr, N.; Vranesic, I.; Kuhn, R. [(3)H]-M-MPEP, A potent, subtype-selective radioligand for the metabotropic glutamate receptor subtype 5. *Bioorg. Med. Chem. Lett.* **2002**, *12* (3), 407–409.

(35) Shanazarov, A. K.; Kuzovkin, V. A.; Chistyakov, V. V.; Granik, V. G. Acetals of lactams and amides. 60. *N*- and *O*-alkylation of 5-oxo-5,6,7,8-tetrahydrocarbostyryils. Synthesis of isoxazolo[5,4-f]- and pyrazolo[3,4-f]quinolines. *Chem. Heterocycl. Compd. (Engl.Transl.)* **1991**, *27* (1), 71–76.

(36) Abu-Shanab, F. A.; Redhouse, A. D.; Thompson, J. R.; Wakefield, B. J. Synthesis of 2,3,5,6-tetrasubstituted pyridines from enamines derived from *N*,*N*-dimethylformamide dimethyl acetal. *Synthesis* **1995**, 557–560.

(37) Baraldi, P. G.; Simoni, D.; Manfredini, S. An improved preparation of enaminones from 1,3-diketones and ammonium acetate or amine acetates. *Synthesis* **1983**, *11*, 902–903.

(38) Ioannis, N.; Molina, A.; Lynch, J.; Reamer, R.; Volante, R.; Reider, P. Condensation of 2-methylbenzoxazole with aromatic aldehydes bearing acidic protons. A convenient coupling in the synthesis of the HIV-reverse transcriptase inhibitor L-696,229. *J. Org. Chem.* **1993**, *58* (11), 3176–3178.

(39) Pettit, G. R.; Fleming, W. C.; Paull, K. D. Synthesis of the 6- and 7-hydroxy-5,8-dioxocarbostyrils. *J. Org. Chem.* **1968**, *33* (3), 1089–1092.

(40) Miyaura, N.; Yanagi, T.; Suzuki, A. The palladium-catalyzed cross-coupling reaction of phenylboronic acid with haloarenes in the presence of bases. *Synth. Commun.* **1981**, *11* (7), 513–519.

(41) Suzuki, A.; Saveda, S.; Saegusa, T. New ring-opening polymerization via a π-allyl complex. 1. Polymerization of diethyl 2-vinylcyclopropane-1,1-dicarboxylate catalyzed by a palladium(0) complex. *Macromolecules* **1989**, *22* (3), 1505–1507.

(42) Gravius, A.; Pietraszek, M.; Schäfer, D.; Schmidt, W. J.; Danysz, W. Effects of mGlu1 and mGlu5 receptor antagonists on negatively reinforced learning. *Behav. Pharmacol.* **2005**, *16* (2), 113–121.

(43) Gasparini, F.; Lingenhohl, K.; Stoehr, N.; Flor, P. J.; Heinrich, M.; Vranesic, I.; Biollaz, M.; Allgeier, H.; Heckendorn, R.; Urwyler, S.; Varney, M. A.; Johnson, E. C.; Hess, S. D.; Rao, S. P.; Sacaan, A. I.; Santori, E. M.; Velicelebi, G.; Kuhn, R. 2-Methyl-6-(phenylethynyl)-pyridine (MPEP), A potent, selective and systemically active mGlu5 receptor antagonist. *Neuropharmacology* **1999**, *38* (10), 1493–1503.

(44) O'Brien, J. A.; Lemaire, W.; Chen, T. B.; Chang, R. S.; Jacobson, M. A.; Ha, S. N.; Lindsley, C. W.; Schaffhauser, H. J.; Sur, C.; Pettibone, D. J.; Conn, P. J., Jr. A family of highly selective allosteric modulators of the metabotropic glutamate receptor subtype 5. *Mol. Pharmacol.* **2003**, *64* (3), 731–740.

(45) Malherbe, P.; Kratochwil, N.; Zenner, M. T.; Piussi, J.; Diener, C.; Kratzeisen, C.; Fischer, C.; Porter, R. H. Mutational analysis and molecular modeling of the binding pocket of the metabotropic glutamate 5 receptor negative modulator 2-methyl-6-(phenylethynyl)-pyridine. *Mol. Pharmacol.* **2003**, *64*, 823–832.

(46) Malherbe, P.; Kratochwil, N.; Knoflach, F.; Zenner, M. T.; Kew, J. N.; Kratzeisen, C.; Maerki, H. P.; Adam, G.; Mutel, V. Mutational analysis and molecular modeling of the allosteric binding site of a novel, selective, noncompetitive antagonist of the metabotropic glutamate 1 receptor. *J. Biol. Chem.* **2003**, *278* (10), 8340–8347.

(47) Jirgensons, A.; Parsons, C. G.; Jaunzeme, I.; Kalvinsh, I.; Henrich, M.; Vanejevs, M.; Kauss, V.; Danysz, W.; Weil, T. Tetrahydroquinolones and their use as modulators of metabotropic glutamate receptors. U.S. Patent 2006004 001, 2006.

(48) Parsons, C. G.; Jirgensons, A.; Jaunzeme, I.; Kalvinsh, I.; Henrich, M.; Vanejevs, M.; Kauss, V.; Danysz, W.; Jatzke, C.; Weil, T., Tetrahydroquinolones and their use as modulators of metabotropic glutamate receptors. Int. Patent WO2007023245, 2007.

(49) Carlier, P. R.; Du, D.-M.; Han, Y.-F.; Liu, J.; Perola, E.; Williams, I. D.; Pang, Y.-P. *Angew. Chem. Int. Ed.* **2000**, *39* (10), 1775–1777; *Angew. Chem.* **2000**, *112*, 1845–1847.

(50) Lowry, O. H. et al. *J. Biol. Chem.* **1951**, *193*, 256–275.

(51) Lipinski, C. A.; Lombardo, F.; Dominy, B. W.; Feeney, P. J. *Adv. Drug Del. Rev.* **2001**, *46*, 3–26.

JM0611298